Symmetry Force Fields for Neutral and Ionic Transition Metal Carbonyl Complexes from Density Functional Theory

Volker Jonas[†] **and Walter Thiel***

Organisch-Chemisches Institut, Universität Zürich, Winterthurerstrasse 190, CH-8057 Zürich, Switzerland

Received: September 3, 1998; In Final Form: December 13, 1998

Symmetry force fields for neutral and ionic transition metal carbonyl complexes have been derived on the basis of gradient-corrected density functional calculations using effective core potential wave functions in conjunction with polarized triple-ζ basis sets. For the neutral carbonyls $[M(CO)_6]$ (M = Cr, Mo, W), $Fe(CO)_5$, and $Ni(CO)_4$, the calculated data are compared to experimentally derived force fields. For three different series of transition metal carbonyl ions, trends in the force fields are discussed in terms of bonding models and electrostatic effects, emphasizing the variation of the calculated results with the total charge of the carbonyl complex. The limitations of the empirical Cotton−Kraihanzel approach are analyzed.

1. Introduction

The experimental determination of complete quadratic force fields in polyatomic molecules is usually limited by insufficient vibrational data. As the number of independent force constants in a molecule is usually much larger than the number of observable frequencies, additional information must be obtained from isotopically substituted species. Such isotopic substitutions are often difficult, and it is sometimes even impossible to generate the required number of isotopomers so that approximations are needed to get complete force fields (e.g., keeping certain interaction elements fixed at reasonable values or allowing them to vary only in a small range around such values). The uncertainties introduced by these simplifying assumptions may be assessed by quantum chemical calculations, which can provide highly accurate values of potential energy constants with only small systematic errors. It is well established, especially for first-row and second-row main-group compounds, that such theoretical symmetry force fields are reliable and useful in supplementing experimental information.[1]

The determination of complete quadratic force fields for characteristic transition metal systems is important for several reasons. Force constants, including interaction constants, are of fundamental interest for a discussion of the bonding between a transition metal and the ligands and may provide additional information about the nature and strength of the transition metal−ligand bonds. It is also relevant to compare the true quadratic force constants with the results of popular approximate treatments such as the Cotton−Kraihanzel (CK) method,[2] where the CO force constants and CO, CO′ interaction constants are obtained from the experimentally observed CO stretching frequencies neglecting all other frequencies and anharmonicity effects ("CO-factored force field").

In continuation of our previous theoretical studies on vibrational spectra of transition metal compounds,[3−7] the present paper reports the symmetry force fields for several series of carbonyl complexes. These are (a) the octahedral (O_h) hexacarbonyls $[M(CO)_6]$ (M = Cr, Mo, W); (b) the trigonal bipyramidal (D_{3h}) pentacarbonyls $[M(CO)_5]$ (M = Fe, Ru, Os); (c) the tetrahedral (T_d) tetracarbonyls $[M(CO)_4]$ (M = Ni, Pd, Pt); (d) the octahedral (O_h) hexacarbonyl ions $[M(CO)_6]^n$ ($n = -1$ for M = V, Nb, Ta; $n = 1$ for M = Mn, Re; $n = 2$ for M = Fe, Ru, Os; $n = 3$ for M = Co, Rh, Ir; $n = 4$ for M = Pt; $n = 5$ for M = Au); (e) the square planar (D_{4h}) tetracarbonyl ions $[M(CO)_4]^n$ ($n = 1$ for M = Co, Rh, Ir; $n = 2$ for M = Ni, Pd, Pt; $n = 3$ for M = Au; $n = 4$ for M = Hg); (f) the linear (D_{4h}) dicarbonyl ions $[M(CO)_2]^n$ ($n = 1$ for M = Au; $n = 2$ for M = Hg; $n = 3$ for M = Tl).

For the neutral carbonyls (a)−(c), our calculated symmetry force fields will be compared with the available experimental data for $[M(CO)_6]$ (M = Cr, Mo, W), $Fe(CO)_5$, and $Ni(CO)_4$. These five neutral carbonyls will serve as validation for the accuracy of our calculated force constants; in addition, the calculated ^{13}CO and $C^{18}O$ isotopic shifts will be compared to experiment, as these shifts form the basis for the experimental force constant determinations.[8−11] Some discrepancies between the calculated and experimental spectra of $Fe(CO)_5$ and $Ni(CO)_4$ will be solved with the help of calculated isotopic shifts and Raman intensities.

For the ionic series (d)−(f), the theoretical force constants will be used to describe systematic trends within the different series of isoelectronic and isostructural carbonyl cations. This extends previous work on the hexacarbonyls (d), which has focused on structures and vibrational frequencies.[5] The analysis of the harmonic force constants and their trends allows a more detailed discussion of the bonding in the carbonyl cations (d)−(f).

The calculated equilibrium geometries, vibrational wavenumbers, and infrared intensities have been or will be presented elsewhere [(a)−(c),[3] (d),[5] (e),[6] (f)[7]]. These data are not given here in order to avoid duplication.

2. Methods of Calculation

The symmetry force fields were computed from the corresponding Cartesian second derivatives using standard transformations.[1] The underlying Cartesian force fields were available from our recent vibrational studies.[3,5−7] Most of the theoretical force fields were obtained from gradient-corrected density functional calculations carried out with the Gaussian94[12]

[†] Present address: San Diego Supercomputer Center, 9500 Gilman Drive, San Diego, CA 92093-0505.

10.1021/jp983600h CCC: $18.00
Published on Web 02/20/1999

program system. Gradient corrections for exchange and for correlation were taken from the work of Becke[13] and Perdew,[14] respectively (usually abbreviated as BP or BP86). Additionally, calculations at the MP2 level[15] were performed for the neutral 4d and 5d complexes. Four basis sets were employed, labeled AE1, AE2, ECP1, and ECP2. AE1 and AE2 use a (14s11p6d)/[8s7p4d] all-electron basis set from Wachters[16] for the 3d transition metal augmented with two additional 4p functions[16] and a diffuse d function.[17] ECP1 and ECP2 use a quasirelativistic effective core potential at the transition metal together with the corresponding (8s7p5d)/[6s5p3d] valence basis set.[18] Thallium is described by the recently published 21ve-ECP combined with a (11s11p8d)/[6s6p4d] valence basis set.[19] For carbon and oxygen, AE1 and ECP1 employ the 6-31G(d) basis,[20] whereas AE2 and ECP2 use a Dunning (10s6p)/[5s3p] triple-ζ basis[21] supplemented by two sets of d polarization functions.[22] Spherical d functions were used throughout.

The molecular geometries were optimized within the given point group symmetry (see above) using analytic energy gradients. Second derivatives were computed analytically at the BP86/AE1 and BP86/AE2 levels.[23] For BP86/ECP1, BP86/ECP2, and MP2/ECP1, second derivatives were obtained by numerical differentiation of the analytic energy gradients. The calculated geometries and harmonic vibrational frequencies have been published elsewhere[3,5] or will be the subject of separate papers.[6,7]

All force field transformations from Cartesian to symmetry coordinates were carried out using the program INTDER.[24] All force constants are given in mdyn Å^{-1} for stretches and stretch−stretch interactions, mdyn rad^{-1} for stretch−bend interactions, and mdyn Å rad^{-2} for bends and bend−bend interactions.

3. Results

In most tables of this paper, we only report BP86/ECP2 data, which are available for all complexes and should generally be more reliable than BP86/ECP1 data due to the larger basis employed. Therefore, comparisons with experiment will normally refer to BP86/ECP2. The other available symmetry force fields (i.e., BP86/ECP1 for all complexes, BP86/AE1 and BP86/AE2 for most of the 3d systems, and MP2/ECP1 for the neutral 4d and 5d carbonyls) are given in the Supporting Information and will be discussed only briefly in a separate section.

In the case of transition metal carbonyl systems, only the anharmonic frequencies are generally available from experiment. Anharmonicity effects normally lower vibrational frequencies (e.g., by 27 cm^{-1} for free CO)[25] and the associate diagonal force constants. This should be kept in mind when comparing theoretical harmonic force constants with experimental values derived from anharmonic frequencies. However, in the region below 900 cm^{-1}, the experimental (anharmonic) and calculated (harmonic) frequencies agree very well[3−5] without correcting for anharmonicity effects so that we may expect a similar correspondence also for the M−C stretching and the bending symmetry force constants.

a. [M(CO)$_6$] (M = Cr, Mo, W). Our previous work on the vibrational spectra of [M(CO)$_6$] (M = Cr, Mo, W) has shown that the calculated structures and harmonic frequencies are very close to experiment.[3] These molecules are the only series of carbonyl complexes where complete empirical symmetry force fields are available, derived from the vibrational spectra of the ^{13}CO and C^{18}O isotopically substituted species.[8]

For octahedral [M(CO)$_6$], the vibrational representation reduces as follows:

$$\Gamma_{vib} = 2A_{1g} + 2E_g + T_{1g} + 4T_{1u} + 2T_{2g} + 2T_{2u}$$

TABLE 1: ^{13}CO and C^{18}O Isotopic Shifts (in cm^{-1}) for M(CO)$_6$ (M = Cr, Mo, W)[a]

			M = Cr		M = Mo		M = W	
			exptl	calcd	exptl	calcd	exptl	calcd
				^{13}CO				
A_{1g}	ν_1	[CO]	48.4	49.5	48.0	50.0	50.2	50.3
A_{1g}	ν_2	[MC]	5.4	6.3	4.4	6.6	4.7[b]	6.8
E_g	ν_3	[CO]	46.0	46.8	46.1	46.6	46.3	46.8
E_g	ν_4	[MC]	6.4	6.6	7.2[b]	6.6	5.2[b]	6.8
T_{1g}	ν_5	[δMCO]	11.2	11.2	9.3	10.3	10.4	10.5
T_{1u}	ν_6	[CO]	44.3	45.0	43.9	44.6	44.1	44.7
T_{1u}	ν_7	[δMCO]	13.3	13.8	15.6	16.6	17.8	18.4
T_{1u}	ν_8	[MC]	7.0	8.8	4.9	5.9	6.0	5.5
T_{1u}	ν_9	[δCMC]	0.7[b]	0.4	0.3	0.3	0.1[b]	0.2
T_{2g}	ν_{10}	[δMCO]	18.3	19.1	16.0	16.6	15.3	16.4
T_{2g}	ν_{11}	[δCMC]	1.3	0.3	0.2	0.3	1.2	0.4
T_{2u}	ν_{12}	[δMCO]	14.5	17.7	15.4	17.5	15.6	17.7
T_{2u}	ν_{13}	[δCMC]		0.4		0.3		0.4
				C^{18}O				
A_{1g}	ν_1	[CO]	46.6	46.1	45.8	45.7	46.2	45.1
A_{1g}	ν_2	[MC]	12.3	14.3	12.0	15.0	15.1[b]	15.7
E_g	ν_3	[CO]	45.3	45.1	45.7	45.3	45.3	44.7
E_g	ν_4	[MC]	14.0	14.4	12.6[b]	14.2	15.0[b]	14.8
T_{1g}	ν_5	[δMCO]	4.8	4.6	4.4	4.5	4.9	4.6
T_{1u}	ν_6	[CO]	47.0	46.5	47.8	47.1	47.0	46.7
T_{1u}	ν_7	[δMCO]	2.3	2.9	2.9	3.1	3.3	3.4
T_{1u}	ν_8	[MC]	10.8	8.9	7.5	8.9	9.9	10.3
T_{1u}	ν_9	[δCMC]	3.6	4.2	3.4	3.5	4.6[b]	3.4
T_{2g}	ν_{10}	[δMCO]	1.4	2.6	3.2	2.8	1.6	2.9
T_{2g}	ν_{11}	[δCMC]	4.9	4.7	4.0	4.1	2.2	4.1
T_{2u}	ν_{12}	[δMCO]	2.8	3.8	3.3	3.7	4.0	3.9
T_{2u}	ν_{13}	[δCMC]	4.6	3.1		2.8		2.9

[a] Gas-phase values unless otherwise noted, ref 8. Calculated values at BP86/ECP2. [b] Solid-state values, ref 8.

Table 1 shows the experimental and calculated ^{13}CO and C^{18}O isotopic shifts for [M(CO)$_6$] (M = Cr, Mo, W); Table 2 contains symmetry and selected internal force constants.

Our calculated isotopic shifts are in very good agreement with the experimental data. The average absolute deviation is 0.8 cm^{-1} with a maximum deviation of 3.2 cm^{-1}. This confirms that the underlying vibrational assignments are correct.[8]

Symmetry coordinates have been taken from ref 8 and are documented in the Supporting Information. The block diagonal force constant matrix contains 13 diagonal elements and a total of 10 nondiagonal coupling elements. The 13 diagonal force constants represent C−O stretching (A_{1g}, E_g, T_{1u}), M−C stretching (A_{1g}, E_g, T_{1u}), M−C−O bending (T_{1g}, T_{1u}, T_{2g}, T_{2u}), and C−M−C bending (T_{1u}, T_{2g}, T_{2u}). Experimentally, harmonic C−O stretching frequencies have been estimated and used for the determination of the C−O force constants, whereas the observed fundamental frequencies were used for the other vibrations.[8]

Figure 1 shows a plot of the calculated versus experimental symmetry force constants for the hexacarbonyls [M(CO)$_6$] (M = Cr, Mo, W; 69 data points), divided into two regions (Figure 1a, C−O stretches; Figure 1b, M−C stretches, all bends and coupling constants). In an overall view, the agreement between the experimental and calculated force constants is good for all three hexacarbonyls. As expected from the calculated C−O stretching frequencies, the calculated C−O force constants F_{11}, F_{33}, and F_{66} are lower than the experimental values by an average of 1.0 mdyn Å^{-1} (see Figure 1a, correlation line shifted by 1.0 mdyn Å^{-1}), which is consistent with an underestimation of the harmonic C−O frequencies (by 51 cm^{-1} on average)[3,8] and an overestimation of the C−O bond length; the order W < Cr < Mo is reproduced quite nicely, although the differences between the three metals are rather small. The calculated M−C

TABLE 2: Harmonic Symmetry Force Constants F_{ij} and Internal Force Constants F_{int} for $M(CO)_6$ (M = Cr, Mo, W)

		$Cr(CO)_6$		$Mo(CO)_6$		$W(CO)_6$	
		exptl[a] (vapor)	BP86 ECP2	exptl[a] (vapor)	BP86 ECP2	exptl[a] (vapor)	BP86 ECP2
A_{1g}	$F_{1,1}$	18.11 ± 0.16	17.08	18.13 ± 0.31	17.05	18.10 ± 0.03	16.95
	$F_{1,2}$	0.38 ± 0.13	0.28	0.36 ± 0.25	0.26	0.36 ± 0.02	0.26
	$F_{2,2}$	2.44 ± 0.02	2.69	2.61 ± 0.04	2.91	3.10 ± 0.01	3.19
E_g	$F_{3,3}$	16.84 ± 0.07	16.08	16.84 ± 0.04	16.11	16.78 ± 0.10	15.99
	$F_{3,4}$	0.69 ± 0.05	0.69	0.68 ± 0.04	0.69	0.82 ± 0.08	0.71
	$F_{4,4}$	2.55 ± 0.01	2.74	2.42 ± 0.01	2.66	2.81 ± 0.01	2.90
T_{1g}	$F_{5,5}$	0.375 ± 0.001	0.38	0.346 ± 0.001	0.34	0.385 ± 0.001	0.36
T_{1u}	$F_{6,6}$	17.22 ± 0.11	16.13	17.39 ± 0.06	16.19	17.21 ± 0.04	16.08
	$F_{6,7}$	0.78 ± 0.13	0.80	0.88 ± 0.07	0.77	0.91 ± 0.06	0.79
	$F_{6,8}$	[0 ± 0.20][b]	0.02	[0 ± 0.20][b]	0.01	[0 ± 0.20][b]	0.01
	$F_{6,9}$	[0 ± 0.50][b]	0.02	[0 ± 0.50][b]	−0.01	[0 ± 0.50][b]	−0.01
	$F_{7,7}$	1.64 ± 0.16	2.00	1.43 ± 0.12	1.68	1.80 ± 0.07	1.87
	$F_{7,8}$	−0.18 ± 0.09	−0.09	−0.07 ± 0.08	−0.05	−0.04 ± 0.06	−0.05
	$F_{7,9}$	[−0.30 ± 0.10][b]	−0.01	[−0.30 ± 0.10][b]	−0.06	[−0.30 ± 0.10][b]	−0.02
	$F_{8,8}$	0.55 ± 0.22	0.50	0.48 ± 0.09	0.48	0.47 ± 0.07	0.50
	$F_{8,9}$	−0.21 ± 0.12	−0.33	−0.30 ± 0.07	−0.36	−0.34 ± 0.04	−0.37
	$F_{9,9}$	0.79 + 0.46/−0.28	0.84	0.83 + 0.25/−0.16	0.81	0.93 + 0.14/−0.09	0.80
T_{2g}	$F_{10,10}$	0.39 ± 0.10	0.41	0.44 ± 0.02	0.37	0.41 ± 0.11	0.38
	$F_{10,11}$	−0.17 ± 0.02	−0.17	−0.11 ± 0.01	−0.14	−0.13 ± 0.05	−0.12
	$F_{11,11}$	0.54 ± 0.16	0.51	0.34 ± 0.02	0.41	0.39 ± 0.14	0.40
T_{2u}	$F_{12,12}$	0.59 ± 0.13	0.48	0.55 ± 0.10	0.46	0.64 ± 0.10	0.49
	$F_{12,13}$	−0.11 ± 0.12	−0.24	−0.19 ± 0.09	−0.29	−0.14 ± 0.10	−0.29
	$F_{13,13}$	0.35 ± 0.12	0.45	0.39 ± 0.13	0.52	0.33 ± 0.10	0.52
	F_{CO}	17.24 ± 0.07[c]	16.27	17.33 ± 0.06[c]	16.30	17.22 ± 0.04[c]	16.20
	F_{MC}	2.08 ± 0.08	2.36	1.96 ± 0.06	2.21	2.36 ± 0.04	2.43
	F_{MCO}	0.48 ± 0.07	0.44	0.45 ± 0.03	0.41	0.48 ± 0.05	0.43
	$F_{CO,CO,cis}$	0.21 ± 0.03[d]	0.17	0.22 ± 0.05[d]	0.16	0.22 ± 0.02[d]	0.16
	$F_{CO,CO,trans}$	0.02 ± 0.07[e]	0.14	−0.06 ± 0.06[e]	0.12	0.00 ± 0.04[e]	0.11
	$F_{MC,MC,cis}$	−0.019 ± 0.003	−0.01	0.031 ± 0.009	0.04	0.049 ± 0.002	0.05
	$F_{MC,MC,trans}$	0.44 ± 0.08	0.36	0.53 ± 0.06	0.54	0.56 ± 0.04	0.57
	$F_{MC,CO}$	0.68 ± 0.07	0.67	0.73 ± 0.06	0.66	0.79 ± 0.04	0.68
	$F_{MC,CO,cis}$	−0.05 ± 0.03	−0.07	−0.05 ± 0.004	−0.07	−0.08 ± 0.02	−0.07
	$F_{MC,CO,trans}$	−0.10 ± 0.07	−0.12	−0.15 ± 0.06	−0.11	−0.12 ± 0.04	−0.11

[a] Reference 8; based on the observed fundamental frequencies, except for the C−O stretching modes where approximate harmonic frequencies have been used; see text for units. [b] Held in the indicated range. [c] Gas-phase data (harm), anharmonic values are 16.74 (Cr), 16.82 (Mo), 16.72 (W) for F_{CO}. [d] Gas-phase data (harm), anharmonic values are 0.21 (Cr), 0.20 (Mo), 0.19 (W) for $F_{CO,CO,cis}$. [e] Gas-phase data (harm), anharmonic values are 0.22 (Cr), 0.12 (Mo), 0.17 (W) for $F_{CO,CO,trans}$.

force constants F_{22}, F_{44}, and F_{77} are slightly higher than the experimental values and show analogous trends (Table 2), with an average deviation of 0.20 mdyn Å^{-1}. In the case of the bending force constants, the average deviations are 0.05 mdyn Å rad^{-2} for M−C−O (12 values) and 0.08 mdyn Å rad^{-2} for C−M−C (nine values).

For all symmetry blocks except T_{1u}, the experimental vibrational data from three isotopic molecules were sufficient to determine all force constants. Within the T_{1u} block, 10 force constants had to be derived from 12 frequencies. "Best estimates" for these 10 force constants were obtained while holding F_{68}, F_{69}, and F_{79} in the ranges given in Table 2. The experimental and theoretical T_{1u} force constants agree quite well, except for F_{79}, which is calculated much closer to zero than to the assumed value of −0.30 ± 0.10 mdyn rad^{-1}. In general, the deviations between the experimental and theoretical force constants are reasonably small for each irreducible representation and also for each of the three hexacarbonyls. Hence, our calculated force constants seem reliable. Since their intrinsic accuracy is the same for all symmetry blocks, they should be preferred over empirical force constants whenever the latter are not well determined (e.g., F_{79}, see above).

Table 2 also contains some selected internal force constants for $[M(CO)_6]$ (M = Cr, Mo, W). Both F_{CO} and F_{MC} show analogous trends in the calculated and experimental values, i.e., W < Cr < Mo for F_{CO} and W > Cr > Mo for F_{MC}, implying that $Mo(CO)_6$ has the strongest C−O and the weakest M−C bond. The empirical interaction force constants $F_{CO,CO,cis}$ and $F_{CO,CO,trans}$ between the C−O stretches are rather sensitive to the experimental input frequencies. $F_{CO,CO,cis}$ is generally found to be around 0.2 mdyn Å^{-1} (gas-phase and solution data, with and without anharmonicity corrections), but $F_{CO,CO,trans}$ is around zero for the harmonic gas-phase data and close to $F_{CO,CO,cis}$ for the anharmonic gas-phase data and the solution data (see Table 2, footnotes d and e).[8] Our calculations yield sizable nonzero values for $F_{CO,CO,trans}$ (0.11−0.14 mdyn Å^{-1}), which are only slightly smaller than those for $F_{CO,CO,cis}$ (0.16−0.17 mdyn Å^{-1}). Neither the empirical nor the experimental values support the qualitative expectation from the CK treatment that the trans interaction constant should be about twice as large as the cis constant.[2]

Theoretical symmetry force constants for $Cr(CO)_6$ and $Ni(CO)_4$ have been given before[26] but are not discussed here since the corresponding DFT calculations yield in both cases an imaginary frequency for a C−M−C bending mode (probably due to numerical inaccuracies). More recent theoretical force fields have not been transformed into symmetry coordinates.[27−29]

b. $[M(CO)_5]$ (M = Fe, Ru, Os). For $[M(CO)_5]$ with D_{3h} symmetry, the vibrational representation reduces as follows:

$$\Gamma_{vib} = 4A_1' + A_2' + 4A_2'' + 6E' + 3E''$$

Table 3 shows the experimental and calculated ^{13}CO and $C^{18}O$ isotopic shifts for $Fe(CO)_5$. Table 4 lists the vibrational

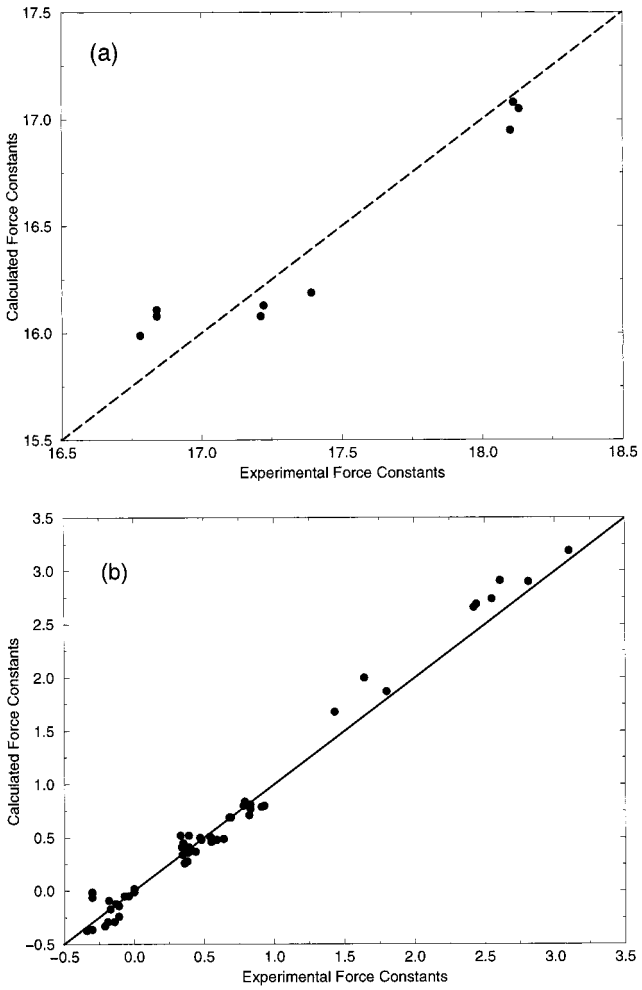

Figure 1. Calculated versus experimental force constants for $[M(CO)_6]$ (M = Cr, Mo, W), divided into two regions (a) (C−O stretches) and (b) (M−C stretches, all bends and coupling constants). The correlation lines with unit slope are shown (shifted by −1 mdyn/Å for (a) and unshifted for (b)); see text for units.

frequencies for $Fe(CO)_5$ at the BP86/ECP2 and BP86/AE1 levels of theory together with the calculated infrared and Raman intensities at BP86/AE1.[30]

As has been discussed in detail previously,[3] we propose to change the original assignment[9] concerning ν_8 (A_2'') and ν_{13} (E') as well as ν_{12} (E') and ν_{16} (E''). This reassignment has also been suggested by others independently.[28] The theoretical isotopic shifts are in very good agreement with the experimental data when these reassignments are taken into account properly (Table 3). Interchanging the experimental isotopic shifts for ν_8 and ν_{13} clearly supports the reassignment of these two M−C stretching frequencies. Furthermore, the new assignments for ν_{12} and ν_{16} (Table 4) imply that the band around 540 cm^{-1} in the infrared probably corresponds to a combination band and that its isotopic shifts[9] are thus irrelevant presently. The calculated ^{13}CO shift of 19.5 cm^{-1} for ν_{16} is the largest of all M−C−O bending values, whereas the shift for $C^{18}O$ is rather small. Also, as ν_{12} is calculated very close to ν_8, the given isotopic shifts for ν_8 are assumed to be valid for ν_{12}, too (Tables 3 and 4). With these assignments, the average absolute deviation between theoretical and experimental shifts is 0.9 cm^{-1}, with a maximum deviation of 2.9 cm^{-1}.

For further validation, we have calculated the Raman intensities for $Fe(CO)_5$ at the BP86/AE1 level of theory by numerical third derivatives with the Gaussian94 program.[12,30] For comparison, the Raman intensities for $Cr(CO)_6$ have also been calculated at the BP86/AE1 level; they are in good agreement with the experimental values; that is, five out of the six active bands have significant intensities, whereas ν_{10} is very weak both in the solid state and the solution spectra and is not seen in the gas-phase Raman spectrum.[31,32] For $Fe(CO)_5$, weak Raman bands are predicted in the middle frequency region for ν_{11}, ν_{13}, ν_{16}, and ν_{17}, whereas ν_3, ν_4, and ν_{12} are stronger. Experimentally, ν_3 and ν_4 have been assigned in the Raman spectrum; also, the band at 493 cm^{-1} may be assigned to ν_{12}. The low theoretical intensities for ν_{11} and ν_{16} imply that the experimental Raman bands around 653 and 555 cm^{-1} may be combination bands, which is also supported by the poor agreement between the infrared and Raman frequencies in these cases and the confusing

TABLE 3: ^{13}CO and $C^{18}O$ Isotopic Shifts (in cm^{-1}) for $Fe(CO)_5$

			^{13}CO exptl[a]	^{13}CO calcd	$C^{18}O$ exptl[a]	$C^{18}O$ calcd
A_1'	ν_1	[CO]	49.5[b]	50.0	46.5[b]	45.2
A_1'	ν_2	[CO]	47.0[b]	47.8	44.3[b]	43.9
A_1'	ν_3	[MC]	6.8[b]	7.2	17.4[b]	16.4
A_1'	ν_4	[MC]	6.5[b]	6.8	13.8[b]	15.6
A_2'	ν_5	[δMCO]	14.0	11.1	4.0	4.4
A_2''	ν_6	[CO]	45.5	46.3	46.5	46.1
A_2''	ν_7	[δMCO]	10.0	10.7	2.8	3.5
A_2''	ν_8	[MC][e]	9.2	11.3	8.1	8.8
A_2''	ν_9	[δCMC]		0.4		4.7
E'	ν_{10}	[CO]	45.4	46.2	45.8	45.1
E'	ν_{11}	[δMCO]	13.8[c]	14.3	3.2[c]	3.4
E'	ν_{12}	[δMCO][e]	9.2	9.9	8.1	10.6
E'	ν_{13}	[MC]	11.5	13.8	4.2	4.2
E'	ν_{14}	[δCMC]	0.5[d]	0.3	6.0[d]	4.2
E'	ν_{15}	[δCMC]	0.4[b]	0.3	4.8[b]	2.5
E''	ν_{16}	[δMCO]		19.5		3.0
E''	ν_{17}	[δMCO]	10.0[b]	11.6	4.0[b]	4.5
E''	ν_{18}	[δCMC]	0.2[b]	0.4	4.6[b]	4.9

[a] Gas-phase values unless otherwise noted; ref 9. Calculated values at BP86/ECP2. [b] Estimated from combination bands. [c] From Table 3 in ref 9; note that the data for ^{13}CO and $C^{18}O$ in Table 7 of ref 9 are wrong. [d] Values from CS_2 solution. [e] ν_8 and ν_{12} are calculated very close; therefore, the published isotopic shifts from ref 9 are adopted for both fundamentals.

TABLE 4: Vibrational Frequencies (in cm^{-1}) and Infrared and Raman Intensities for $Fe(CO)_5$

			exptl ν_i[a] (vapor)	BP86 ECP2	$\Delta\nu$	BP86 AE1	int.[b] infrared	int.[b] Raman
A_1'	ν_1	[CO]	2120.7[c]	2090	−31	2098		54.3
A_1'	ν_2	[CO]	2041.7[c]	2012	−30	2028		116.0
A_1'	ν_3	[MC]	442.8[c]	453	10	455		11.9
A_1'	ν_4	[MC]	413.4[c]	428	15	431		35.2
A_2'	ν_5	[δMCO]	383	361	−22	356		
A_2''	ν_6	[CO]	2034.0	2011	−23	2024	1128.8	
A_2''	ν_7	[δMCO]	618.8	621	2	621	127.7	
A_2''	ν_8	[MC]	475.3	485	10	487	0.1	
A_2''	ν_9	[δCMC]	100[d]	104	4	106	0.3	
E'	ν_{10}	[CO]	2013.3	1990	−23	2008	1909.2	98.7
E'	ν_{11}	[δMCO]	645.0	657	12	658	250.9	1.3
E'	ν_{12}	[δMCO]	493[f]	489	−4	492	0.7	4.1
E'	ν_{13}	[MC]	429.0	436	7	431	10.4	0.1
E'	ν_{14}	[δCMC]	104.9	100	−5	101	0.1	4.2
E'	ν_{15}	[δCMC]	74.3[c]	50	−24	53	0	4.5
E''	ν_{16}	[δMCO]	552.8[e]	552	−1	544		0.2
E''	ν_{17}	[δMCO]	375[c]	374	−1	368		0
E''	ν_{18}	[δCMC]	97.3[c]	93	−4	94		14.0

[a] Reference 9, assignments ν_8/ν_{13} and ν_{12}/ν_{16} reversed (see text). [b] Infrared intensities in km/mol, Raman intensities in $Å^4$/amu, both from BP86/AE1; see ref 30. [c] Estimated from combination bands. [d] Estimate based on ν_{14} and ν_{18}, quoted uncertainty of 15 cm^{-1}. [e] Values from CS_2 solution (Raman).

isotopic shifts.[9] The low theoretical intensities for ν_{13} and ν_{17} are consistent with experiment; that is, no further Raman band close to ν_4 has been observed and ν_{17} has only been assigned from combination bands.[9] Thus, both the calculated isotopic shifts and Raman intensities clearly support the new assignments for $Fe(CO)_5$.

Table 5 contains the symmetry and selected internal force constants for $[M(CO)_5]$ (M = Fe, Ru, Os).

Symmetry coordinates have been taken from ref 9 and are also given in the Supporting Information. The block diagonal force constant matrix contains 18 diagonal elements and a total of 30 nondiagonal coupling elements. In the case of $Fe(CO)_5$, a complete empirical symmetry force field has been published[9] that is based on the vibrational spectra of three isotopomers (with anharmonicity corrections for the C−O stretching frequencies only) and relies on a large number of constraints.[9] Moreover, the empirical force field makes use of the original incorrect assignments for ν_8, ν_{12}, ν_{13}, and ν_{16} (see above) and is therefore unreliable in the A_2'', E′, and E″ blocks. Meaningful comparisons between theory and experiment are thus restricted to the A_1' and A_2' blocks where we generally find reasonable agreement (see Table 5). The two C−O stretching force constants F_{11} and F_{22} are lower than the experimental values, as expected from the corresponding frequencies. In the case of the two M−C stretching force constants, the order of F_{33} and F_{44} is reversed, which is surprising. For the six interaction elements, both the signs and the relative magnitudes agree well, but it should be kept in mind that four of the experimental values were estimated from analogous constants for the hexacarbonyls.

Further comparisons between theory and experiment are possible for some internal force constants for $Fe(CO)_5$ and $Ru(CO)_5$ (Table 5). In the latter case, the experimental values come from a study of the infrared active C−O frequencies for the compounds $Ru(CO)_{5-x}(^{13}CO)_x$ ($x = 0-5$) in liquid xenon solution[33] where internal C−O valence force constants were determined from the C−O frequencies for 12 isotopically substituted molecules (CK treatment). Experiment and theory agree with regard to the order $F_{CO,ax} > F_{CO,eq}$. However, the trends in the three $F_{CO,CO}$ coupling elements are not the same; experimentally, the axial interaction element should be largest, whereas theoretically this element is rather small. In this case, the theoretical values are expected to be more reliable in view of the limitations in the experimental investigations (wrong assignments for $Fe(CO)_5$, CK values for $Ru(CO)_5$).

Turning to comparisons between the theoretical results, the symmetry force fields for the three pentacarbonyls are quite similar; both the four C−O and the four M−C stretching force constants show the same order. $Ru(CO)_5$ tends to have the highest C−O stretching, the lowest M−C stretching, and the lowest M−C−O bending force constants. Considering the internal force constants, F_{CO} and F_{MC} are always predicted to be larger for the axial ligands, and the M−C force constants are significantly larger in the pentacarbonyls than in the hexacarbonyls, which indicates stronger M−C bonds in the d^8 systems compared with the d^6 systems.

c. $[M(CO)_4]$ (M = Ni, Pd, Pt). For tetrahedral $[M(CO)_4]$, the vibrational representation reduces as follows:

$$\Gamma_{vib} = 2A_1 + 2E + 4T_2 + T_1$$

Table 6 shows the experimental and calculated ^{13}CO and $C^{18}O$ isotopic shifts for $Ni(CO)_4$. The agreement between the experimental and our calculated ^{13}CO and $C^{18}O$ isotopic shifts is about as good as that for the other carbonyls (see above), with an average absolute deviation of 0.9 cm^{-1} and a maximum deviation of 2.8 cm^{-1}. Table 7 lists the vibrational frequencies for $Ni(CO)_4$ at the BP86/ECP2 and BP86/AE1 levels of theory together with the calculated infrared and Raman intensities at BP86/AE1.

TABLE 5: Harmonic Symmetry Force Constants F_{ij} and Internal Force Constants F_{int} for $M(CO)_5$ (M = Fe, Ru, Os)

		$Fe(CO)_5$		$Ru(CO)_5$		$Os(CO)_5$
		exptl[a] (vapor)	BP86 ECP2	exptl[b] (liq Xe)	BP86 ECP2	BP86 ECP2
A_1'	$F_{1,1}$	17.27	16.43		16.37	16.19
	$F_{1,2}$	0.35	0.47		0.43	0.44
	$F_{1,3}$	0.60	0.51		0.55	0.60
	$F_{1,4}$	−0.28	−0.20		−0.21	−0.22
	$F_{2,2}$	17.86	16.59		16.76	16.70
	$F_{2,3}$	−0.31	−0.15		−0.15	−0.15
	$F_{2,4}$	0.65	0.57		0.55	0.57
	$F_{3,3}$	3.20	3.20		3.11	3.65
	$F_{3,4}$	−0.19	−0.12		0.10	0.14
	$F_{4,4}$	3.02	3.43		3.58	3.96
A_2'	$F_{5,5}$	0.40	0.36		0.31	0.36
A_2''	$F_{6,6}$	17.46	16.40		16.63	16.58
	$F_{6,7}$	0.00	0.03		0.05	0.06
	$F_{6,8}$	0.84	0.75		0.71	0.73
	$F_{6,9}$	0.08	0.02		0.12	0.15
	$F_{7,7}$	0.32	0.40		0.33	0.37
	$F_{7,8}$	−0.08	−0.10		−0.09	−0.10
	$F_{7,9}$	−0.14	0.21		0.25	0.29
	$F_{8,8}$	2.17	2.39		2.01	2.24
	$F_{8,9}$	−0.23	−0.06		−0.07	−0.13
	$F_{9,9}$	0.85	0.83		0.90	0.96
E′	$F_{10,10}$	17.1	15.97		15.99	15.81
	$F_{10,11}$	−0.3	0.00		0.00	0.00
	$F_{10,12}$	−0.1	0.06		0.09	0.09
	$F_{10,13}$	0.9	0.73		0.69	0.73
	$F_{10,14}$	0.7	0.03		−0.02	−0.03
	$F_{10,15}$	−0.2	0.07		0.11	0.12
	$F_{11,11}$	0.6	0.51		0.49	0.52
	$F_{11,12}$	0.0	0.02		0.03	0.03
	$F_{11,13}$	−0.2	−0.02		0.02	0.00
	$F_{11,14}$	−0.2	−0.24		−0.31	−0.33
	$F_{11,15}$	0.1	0.06		0.06	0.05
	$F_{12,12}$	0.6	0.42		0.39	0.43
	$F_{12,13}$	−0.1	−0.16		−0.20	−0.20
	$F_{12,14}$	−0.1	−0.13		−0.16	−0.16
	$F_{12,15}$	0.1	0.12		0.11	0.09
	$F_{13,13}$	2.4	2.58		2.24	2.65
	$F_{13,14}$	0.0	0.00		−0.02	0.05
	$F_{13,15}$	0.1	−0.03		0.00	0.04
	$F_{14,14}$	0.6	0.74		0.87	0.93
	$F_{14,15}$	−0.2	−0.23		−0.25	−0.26
	$F_{15,15}$	0.4	0.23		0.20	0.19
E″	$F_{16,16}$	0.38	0.48		0.45	0.47
	$F_{16,17}$	0.00	−0.03		−0.03	−0.02
	$F_{16,18}$	−0.04	−0.14		−0.12	−0.11
	$F_{17,17}$	0.42	0.37		0.27	0.30
	$F_{17,18}$	−0.06	0.09		0.06	0.05
	$F_{18,18}$	0.47	0.53		0.46	0.46
	$F_{CO,ax}$	17.43	16.49	17.28	16.70	16.64
	$F_{CO,eq}$	16.47	16.13	16.53	16.12	15.94
	$F_{MC,ax}$	2.57	2.91		2.80	3.10
	$F_{MC,eq}$	2.64	2.79		2.53	2.98
	$F_{MCO,ax-eq}$		0.49		0.47	0.49
	$F_{MCO,eq-ax}$		0.38		0.29	0.32
	$F_{MCO,eq-eq}$		0.40		0.36	0.40
	$F_{CO,CO,ax-ax}$	0.33	0.09	0.48	0.06	0.06
	$F_{CO,CO,ax-eq}$	0.14	0.19	0.28	0.17	0.18
	$F_{CO,CO,eq-eq}$	0.12	0.15	0.35	0.13	0.13

[a] Reference 9; based on the observed fundamental frequencies, except for the C−O stretching modes where approximate harmonic frequencies have been used. Solution values are given for the E″ block; see text for units. [b] Reference 33, based on observed CO frequencies.

TABLE 6: ^{13}CO and $C^{18}O$ Isotopic Shifts (in cm^{-1}) for $Ni(CO)_4$[a]

			^{13}CO exptl	^{13}CO calcd	$C^{18}O$ exptl	$C^{18}O$ calcd
A_1	ν_1	[CO]	49.1	49.3	46.5	46.6
A_1	ν_2	[MC]	3.6	6.2	10.9	13.7
E	ν_3	[δMCO]		16.5		2.9
E	ν_4	[δCMC]	0.0[b]	0.3	4.0[b]	3.1
T_2	ν_5	[CO]	46.6	46.8	47.4	46.5
T_2	ν_6	[δMCO]	16.2	13.9	5.1	5.5
T_2	ν_7	[MC]	5.8	5.4	6.5	7.2
T_2	ν_8	[δCMC]	0.0[c]	0.2	3.0[c]	3.2
T_1	ν_9	[δMCO]	10.0[d]	8.7		3.5

[a] Gas-phase values unless otherwise noted; ref 11a. Calculated values at BP86/ECP2. [b] Values from CCl_4 solution. [c] Uncertain values from $(\nu_5)_{obs} - (\nu_5 - \nu_8)_{obs}$. [d] Solution value from $2\nu_9$.

TABLE 7: Vibrational Frequencies (in cm^{-1}) and Infrared and Raman Intensities for $Ni(CO)_4$

			exptl ν_i[a] (vapor)	BP86 ECP2	$\Delta\nu$	BP86 AE1	int.[b] infrared	int.[b] Raman
A_1	ν_1	[CO]	2132.4	2093	−39	2101		55.3
A_1	ν_2	[MC]	370.8	383	12	390		21.9
E	ν_3	[δMCO]		471		466		0.9
E	ν_4	[δCMC]	62	61	−1	61		10.7
T_2	ν_5	[CO]	2057.8	2026	−32	2041	2276.1	245.5
T_2	ν_6	[δMCO]	458.9	467	8	468	9.2	6.5
T_2	ν_7	[MC]	423.1	438	15	448	164.3	0.2
T_2	ν_8	[δCMC]	80	77	−3	75	0.0	7.9
T_1	ν_9	[δMCO]	300[c]	286	−14	279		

[a] References 10 and 11. [b] Infrared intensities in km/mol, Raman intensities in $Å^4$/amu, both from BP86/AE1. [c] From solution value for $2\nu_9$.

The vibrational spectrum of $Ni(CO)_4$ has been discussed in detail in previous publications.[3,26,28] As pointed out by several authors,[26,28,34] the experimentally estimated frequency of 380 cm^{-1} for the E-type M−C−O bending vibration ν_3 is incompatible with the theoretical calculations. For all other vibrations, the differences between the calculated and the experimental frequencies are in the usual range (Table 7).[3] Experimentally, the infrared spectrum shows two bands for ν_6 and ν_7 at 459 and 423 cm^{-1}, with the latter one being much more intense, which is in accordance with the calculated infrared intensities (Table 7).[10] Previous work[35] has observed a Raman band at 461 cm^{-1}, which might represent both ν_3 (only Raman active) and ν_6 (infrared and Raman active) since our calculations predict almost equal frequencies for these two modes. For further clarification, we have computed the Raman intensities for $Ni(CO)_4$ at the BP86/AE1 level analogous to $Cr(CO)_6$ (Table 7). The calculations suggest that ν_3 should yield a very weak Raman band (comparable to ν_7 and much weaker than ν_2 or ν_6) so that it should be quite difficult to identify ν_3 in the Raman spectrum of $Ni(CO)_4$.

Table 8 contains symmetry and selected internal force constants for $[M(CO)_4]$ (M = Ni, Pd, Pt).

The complete symmetry coordinates have been taken from ref 10. The block diagonal force constant matrix contains nine diagonal elements and a total of eight nondiagonal coupling elements. The experimental quadratic force field for $Ni(CO)_4$ has been refined by Hedberg et al.[10] based on vibrational data from Jones et al., who have also reported a harmonic force field based on a comprehensive analysis of the vibrational spectra of three isotopic species.[11] Both sets of experimentally derived symmetry force constants are given in Table 8, together with our calculated data. Since ν_3 has most likely been incorrectly assigned previously (see above),[10,11] the empirical force constants in the E block are questionable. For the other symmetry blocks, the agreement between the experimental and theoretical symmetry force constants is satisfactory (Table 8). Our calculations show sizable values for the interaction constants $F_{3,4}$ (0.16) and $F_{7,8}$ (0.17), which were set to zero in the more recent experimental refinement of Hedberg.[10]

TABLE 8: Harmonic Symmetry Force Constants F_{ij} and Internal Force Constants F_{int} for $M(CO)_4$ (M = Ni, Pd, Pt)

		$Ni(CO)_4$			$Pd(CO)_4$	$Pt(CO)_4$
		exptl[a,b] (vapor)	exptl[a,c] (vapor)	BP86 ECP2	BP86 ECP2	BP86 ECP2
A_1	$F_{1,1}$	18.233 ± 0.333	18.22 ± 0.09	17.21	17.24	17.00
	$F_{1,2}$	0.235 ± 0.272	0.23 ± 0.07	0.30	0.34	0.46
	$F_{2,2}$	2.355 ± 0.037	2.36 ± 0.02	2.50	2.01	2.82
E	$F_{3,3}$	0.342	0.43 ± 0.05	0.34	0.23	0.32
	$F_{3,4}$	[0][d]	0.09 ± 0.03	0.16	0.13	0.13
	$F_{4,4}$	0.151	0.08 ± 0.02	0.31	0.24	0.22
T_2	$F_{5,5}$	17.867 ± 0.349	17.73 ± 0.12	16.52	16.69	16.43
	$F_{5,6}$	0.740 ± 0.295	0.62 ± 0.13	0.58	0.50	0.58
	$F_{5,7}$	[0][d]	[0.0 ± 0.2][e]	−0.04	−0.04	−0.06
	$F_{5,8}$	[0][d]	[0.0 ± 0.2][e]	−0.05	−0.08	−0.13
	$F_{6,6}$	2.013 ± 0.046	1.98 ± 0.14	2.18	1.62	2.19
	$F_{6,7}$	0.126 ± 0.021	−0.10 ± 0.14	0.21	0.24	0.31
	$F_{6,8}$	0.223 ± 0.031	[0.2 ± 0.1][e]	0.26	0.31	0.40
	$F_{7,7}$	0.486 ± 0.006	0.60 ± 0.11	0.29	0.19	0.26
	$F_{7,8}$	[0][d]	[0.1 ± 0.1][e]	0.17	0.16	0.19
	$F_{8,8}$	0.221 ± 0.007	0.21 ± 0.05	0.45	0.46	0.55
T_1	$F_{9,9}$	0.238 ± 0.001	0.248	0.22	0.12	0.19
	F_{CO}[f]		17.85 ± 0.09	16.70	16.83	16.58
	F_{MC}		2.08 ± 0.10	2.26	1.72	2.34
	F_{MCO}		0.31 ± 0.08	0.28	0.17	0.25
	$F_{CO,CO}$[g]		0.12 ± 0.04	0.17	0.14	0.14

[a] Based on the observed fundamental frequencies, except for the C−O stretching modes where approximate harmonic frequencies have been used. See text for units. [b] Reference 10. [c] Reference 11. [d] Fixed values. [e] Held in the indicated range. [f] Reference 36: 17.23 (Ni), 17.48 (Pd), 17.25 (Pt); CK treatment, CO matrix. [g] Reference 36: 0.37 (Ni), 0.24 (Pd), 0.30 (Pt); CK treatment, CO matrix.

Approximate CK force constants have been derived from matrix spectra of $Ni(CO)_4$, $Pd(CO)_4$, and $Pt(CO)_4$ (Table 8, footnotes f and g). The values for F_{CO} seem reasonable, while those for $F_{CO,CO}$ are considerably higher and probably less reliable than the theoretical values (and the gas-phase value for $Ni(CO)_4$). A comparison of the theoretical results indicates that the 4d species $Pd(CO)_4$ has the highest C−O and the lowest M−C and M−C−O force constants, analogous to $Ru(CO)_5$ and $Mo(CO)_6$ (see above).

d. $[M(CO)_6]^n$ ($n = -1$ for M = V, Nb, Ta; $n = 1$ for M = Mn, Re; $n = 2$ for M = Fe, Ru, Os; $n = 3$ for M = Co, Rh, Ir; $n = 4$ for M = Pt; $n = 5$ for M = Au). Table 9 contains the calculated symmetry and selected internal force constants for the 3d and 4d hexacarbonyl ions; Table 10 lists the corresponding data for the 5d systems including neutral $W(CO)_6$.

In general, the force constants within each group are very similar. The variation of several calculated properties with the total charge of the hexacarbonyls has been discussed in our previous paper[5] and, partly also, in three other recent papers.[37−39] In section 4, we will extend our previous discussion to the complete symmetry force fields for the series $[Ta(CO)_6]^-$ to $[Au(CO)_6]^{5+}$ (Table 10) and provide comparisons with the data for the other two series of carbonyl cations (e) and (f).

e. $[M(CO)_4]^n$ ($n = 1$ for M = Co, Rh, Ir; $n = 2$ for M = Ni, Pd, Pt; $n = 3$ for M = Au; $n = 4$ for M = Hg). For square planar $[M(CO)_4]^n$, the vibrational representation reduces as follows:

TABLE 9: Harmonic Symmetry Force Constants F_{ij} and Internal Force Constants F_{int} for the 3d and 4d Ions $[M(CO)_6]^n$ (M = V, Nb; Mn; Fe, Ru; Co, Rh; $n = -1$ to 3, Respectively)[a]

		V	Nb	Mn	Fe	Ru	Co	Rh
A_{1g}	$F_{1,1}$	15.56	15.54	18.42	19.41	19.44	19.92	20.01
	$F_{1,2}$	0.30	0.27	0.25	0.19	0.16	0.09	0.06
	$F_{2,2}$	2.53	2.53	2.54	2.21	2.75	1.84	2.29
E_g	$F_{3,3}$	14.21	14.27	17.80	19.14	19.16	19.86	19.94
	$F_{3,4}$	0.62	0.61	0.63	0.45	0.47	0.20	0.22
	$F_{4,4}$	2.64	2.38	2.50	2.11	2.38	1.72	1.98
T_{1g}	$F_{5,5}$	0.39	0.34	0.35	0.31	0.31	0.28	0.28
T_{1u}	$F_{6,6}$	14.29	14.39	17.83	19.16	19.20	19.88	19.96
	$F_{6,7}$	0.74	0.70	0.71	0.48	0.49	0.23	0.23
	$F_{6,8}$	0.02	0.01	0.02	0.02	0.01	0.01	0.01
	$F_{6,9}$	0.00	−0.02	0.02	0.03	0.00	0.04	0.02
	$F_{7,7}$	2.06	1.66	1.70	1.40	1.28	1.23	1.16
	$F_{7,8}$	−0.10	−0.05	−0.07	−0.04	−0.03	−0.01	−0.01
	$F_{7,9}$	−0.06	−0.08	0.05	0.10	0.06	0.12	0.11
	$F_{8,8}$	0.53	0.49	0.43	0.37	0.37	0.31	0.31
	$F_{8,9}$	−0.33	−0.35	−0.28	−0.20	−0.27	−0.12	−0.17
	$F_{9,9}$	0.61	0.56	0.99	1.04	1.14	0.96	1.12
T_{2g}	$F_{10,10}$	0.41	0.36	0.39	0.35	0.33	0.31	0.29
	$F_{10,11}$	−0.17	−0.13	−0.15	−0.12	−0.10	−0.08	−0.07
	$F_{11,11}$	0.41	0.31	0.57	0.59	0.51	0.56	0.49
T_{2u}	$F_{12,12}$	0.51	0.48	0.43	0.36	0.37	0.31	0.31
	$F_{12,13}$	−0.23	−0.27	−0.22	−0.17	−0.23	−0.11	−0.16
	$F_{13,13}$	0.29	0.34	0.58	0.66	0.78	0.62	0.78
	F_{CO}	14.47	14.54	17.92	19.20	19.22	19.88	19.96
	F_{MC}	2.33	2.04	2.11	1.77	1.89	1.49	1.62
	F_{MCO}	0.46	0.42	0.40	0.35	0.35	0.30	0.30
	$F_{CO,CO,cis}$	0.23	0.21	0.10	0.05	0.05	0.01	0.01
	$F_{CO,CO,trans}$	0.19	0.15	0.09	0.03	0.03	0.00	0.00

[a] Calculated at BP86/ECP2; see text for units.

TABLE 10: Harmonic Symmetry Force Constants F_{ij} and Internal Force Constants F_{int} for the 5d Complexes $[M(CO)_6]^n$ (M = Ta, W, Re, Os, Ir, Pt, Au; $n = -1$ to 5, Respectively)[a]

		Ta	W	Re	Os	Ir	Pt	Au
A_{1g}	$F_{1,1}$	15.47	16.95	18.30	19.36	20.02	20.11	19.54
	$F_{1,2}$	0.27	0.26	0.24	0.18	0.09	−0.03	−0.13
	$F_{2,2}$	2.72	3.19	3.34	3.16	2.78	2.17	1.11
E_g	$F_{3,3}$	14.18	15.99	17.68	19.05	19.91	20.09	19.49
	$F_{3,4}$	0.62	0.71	0.69	0.53	0.29	0.03	−0.22
	$F_{4,4}$	2.56	2.90	2.94	2.71	2.35	1.79	0.72
T_{1g}	$F_{5,5}$	0.36	0.36	0.35	0.33	0.30	0.28	0.25
T_{1u}	$F_{6,6}$	14.31	16.08	17.75	19.09	19.94	20.11	19.50
	$F_{6,7}$	0.71	0.79	0.74	0.55	0.29	0.08	−0.06
	$F_{6,8}$	0.00	0.01	0.01	0.01	0.01	0.00	0.00
	$F_{6,9}$	−0.03	−0.01	0.00	0.00	0.01	0.03	0.01
	$F_{7,7}$	1.81	1.87	1.73	1.47	1.34	1.27	0.89
	$F_{7,8}$	−0.06	−0.05	−0.05	−0.04	−0.02	−0.01	−0.01
	$F_{7,9}$	−0.05	−0.02	0.03	0.09	0.14	0.17	0.15
	$F_{8,8}$	0.51	0.50	0.46	0.40	0.35	0.30	0.27
	$F_{8,9}$	−0.34	−0.37	−0.35	−0.30	−0.22	−0.13	−0.05
	$F_{9,9}$	0.56	0.80	1.04	1.21	1.27	1.19	0.96
T_{2g}	$F_{10,10}$	0.36	0.38	0.38	0.35	0.32	0.29	0.26
	$F_{10,11}$	−0.12	−0.12	−0.12	−0.10	−0.07	−0.04	−0.01
	$F_{11,11}$	0.31	0.40	0.48	0.52	0.53	0.50	0.42
T_{2u}	$F_{12,12}$	0.50	0.49	0.45	0.40	0.35	0.30	0.26
	$F_{12,13}$	−0.26	−0.29	−0.29	−0.25	−0.20	−0.13	−0.06
	$F_{13,13}$	0.34	0.52	0.71	0.85	0.91	0.86	0.63
	F_{CO}	14.46	16.20	17.82	19.13	19.94	20.10	19.50
	F_{MC}	2.21	2.43	2.40	2.16	1.92	1.60	0.87
	F_{MCO}	0.43	0.43	0.41	0.37	0.33	0.29	0.26
	$F_{CO,CO,cis}$	0.22	0.16	0.10	0.05	0.02	0.00	0.00
	$F_{CO,CO,trans}$	0.15	0.11	0.07	0.03	0.00	−0.01	−0.01

[a] Calculated at BP86/ECP2. To facilitate comparisons, the calculated data for $[W(CO)_6]$ from Table 2 are reproduced here; see text for units.

$$\Gamma_{vib} = 2A_{1g} + A_{2g} + 2A_{2u} + 2B_{1g} + 2B_{2g} + 2B_{2u} + E_g + 4E_u$$

Table 11 contains the calculated symmetry and selected internal force constants for the tetracarbonyl ions.[6]

The force constants within each group are again very similar, thus the discussion in section 4 will focus on the 5d complexes (M = Ir, Pt, Au, Hg; Table 11). For the sake of completeness, we have also included the data for $[Co(CO)_4]^+$, although this species most probably has a triplet ground state.[6,40] The structures, harmonic frequencies, and isotopic shifts of the tetracarbonyl series are discussed in a separate paper.[6]

f. $[M(CO)_2]^n$ ($n = 1$ for M = Au; $n = 2$ for M = Hg; $n = 3$ for M = Tl). For linear $[M(CO)_2]^n$, the vibrational representation reduces as follows:

$$\Gamma_{vib} = 2\Sigma_g^+ + 2\Sigma_u^+ + \Pi_g + 2\Pi_u$$

Table 12 compares the calculated and experimental ^{13}CO and $C^{18}O$ isotopic shifts for $[Au(CO)_2]^+$. Table 13 contains the calculated symmetry and selected internal force constants for the linear dicarbonyl ions together with experimental data for $[Au(CO)_2]^+$.[7,47]

Even though the analogous complexes $[Cu(CO)_2]^+$ and $[Ag(CO)_2]^+$ are also known experimentally,[42−44] we will concentrate on $[Au(CO)_2]^+$, which is the only ion studied presently where complete isotopic data are available both for the ^{13}CO and the $C^{18}O$ substituted species.[41] The differences between the experimental and theoretical isotopic shifts are similar as for the neutral carbonyls, with an average absolute deviation of 0.9 cm^{-1} and a maximum deviation of 4.6 cm^{-1}. The experimental symmetry force constants for $[Au(CO)_2]^+$ have been calculated from the internal force constants in ref 41b.[45] They agree reasonably well with the theoretical values, with one exception. The calculations underestimate the C−M−C bending frequency ν_7 from the solid-state spectra and therefore also the associate force constant F_{77} in $[Au(CO)_2]^+$. The force fields of the complete $[M(CO)_2]^n$ series are described elsewhere together with those for the corresponding $[M(CN)_2]^n$ series (M = Au, Hg, Tl).[7]

g. Force Fields from Theoretical Levels Other Than BP86/ECP2. Other theoretical force fields have also been generated, i.e., BP86/ECP1 for all complexes, BP86/AE1 and BP86/AE2 for the neutral 3d complexes and the hexacarbonyl 3d ions, and MP2/ECP1 for the neutral 4d and 5d complexes. These data are collected in Tables S6−S11 of the Supporting Information and will be summarized briefly here.

Figure 2 displays the BP86/ECP2 versus the BP86/ECP1 force constants for all molecules from the series (a−e) (779 data points), divided into two regions (Figure 2a, C−O stretches; Figure 2b, M−C stretches, all bends and coupling constants).

For the latter region, the agreement is excellent. However, for the C−O stretching region, the plot would afford a correlation line with a slope slightly higher than 1 (Figure 2a). This may be rationalized by considering the effects of enlarging the ligand basis from 6-31G(d) (ECP1) to TZ2P (ECP2) while keeping the metal basis constant; in the anions $[M(CO)_6]^-$ (low CO force constants), the larger ligand basis enhances back-donation to the CO ligand and thus favors lower C−O force constants at BP86/ECP2. On the other hand, in the highly charged cations $[M(CO)_6]^n$ ($n = 3-5$) with high force constants, enlargement of the ligand basis may lead to a better description of the covalent C−O bonding and thus to higher C−O force constants at BP86/ECP2.

When plotting the BP86/AE1 and BP86/AE2 force constants versus the respective BP86/ECP1 and BP86/ECP2 force con-

TABLE 11: Harmonic Symmetry Force Constants F_{ij} and Internal Force Constants F_{int} for the Complexes $[M(CO)_4]^n$ (M = Co, Rh, Ir; Ni, Pd, Pt; Au; Hg; n = 1 to 4, respectively)[a]

		Co	Rh	Ir	Ni	Pd	Pt	Au	Hg
A_{1g}	$F_{1,1}$	18.60	18.76	18.66	19.82	19.92	19.87	20.29	19.65
	$F_{1,2}$	0.27	0.23	0.28	0.14	0.09	0.15	−0.03	−0.17
	$F_{2,2}$	2.75	3.08	3.79	2.11	2.37	3.08	2.19	0.78
A_{2g}	$F_{3,3}$	0.32	0.29	0.33	0.28	0.26	0.30	0.26	0.23
A_{2u}	$F_{4,4}$	0.34	0.34	0.41	0.28	0.28	0.33	0.27	0.22
	$F_{4,5}$	−0.08	−0.10	−0.15	−0.07	−0.09	−0.13	−0.08	−0.02
	$F_{5,5}$	0.03	0.09	0.14	0.17	0.22	0.29	0.32	0.23
B_{1g}	$F_{6,6}$	18.17	18.41	18.29	19.72	19.83	19.75	20.28	19.60
	$F_{6,7}$	0.56	0.55	0.63	0.28	0.26	0.36	0.05	−0.22
	$F_{7,7}$	2.82	2.75	3.42	2.08	2.03	2.69	1.90	0.58
B_{2g}	$F_{8,8}$	0.37	0.33	0.37	0.31	0.29	0.32	0.28	0.23
	$F_{8,9}$	−0.14	−0.12	−0.11	−0.09	−0.07	−0.08	−0.04	0.01
	$F_{9,9}$	0.59	0.51	0.54	0.54	0.46	0.53	0.48	0.36
B_{2u}	$F_{10,10}$	0.35	0.35	0.41	0.29	0.29	0.34	0.27	0.22
	$F_{10,11}$	−0.09	−0.12	−0.15	−0.08	−0.10	−0.13	−0.09	−0.06
	$F_{11,11}$	0.03	0.08	0.07	0.14	0.19	0.21	0.25	0.15
E_g	$F_{12,12}$	0.28	0.28	0.32	0.25	0.25	0.28	0.25	0.21
E_u	$F_{13,13}$	18.17	18.42	18.31	19.73	19.84	19.77	20.30	19.62
	$F_{13,14}$	0.73	0.65	0.73	0.33	0.27	0.38	0.07	−0.10
	$F_{13,15}$	0.00	0.01	0.01	0.00	0.01	0.00	0.00	−0.01
	$F_{13,16}$	0.08	0.02	0.02	0.05	0.01	0.01	0.02	0.02
	$F_{14,14}$	1.63	1.44	1.77	1.37	1.26	1.51	1.47	0.91
	$F_{14,15}$	0.00	0.03	0.00	0.01	0.02	0.00	0.00	−0.01
	$F_{14,16}$	−0.11	−0.12	−0.04	−0.03	−0.05	0.01	0.08	0.12
	$F_{15,15}$	0.39	0.35	0.41	0.31	0.29	0.34	0.29	0.24
	$F_{15,16}$	−0.21	−0.25	−0.30	−0.12	−0.16	−0.21	−0.12	−0.03
	$F_{16,16}$	0.78	0.90	1.01	0.77	0.89	1.08	0.98	0.65
	F_{CO}	18.28	18.50	18.39	19.75	19.86	19.79	20.29	19.62
	F_{MC}	2.21	2.18	2.69	1.73	1.73	2.20	1.76	0.80
	F_{MCO}	0.37	0.33	0.38	0.30	0.28	0.32	0.28	0.24
	F'_{MCO}	0.31	0.31	0.37	0.27	0.27	0.31	0.26	0.22
	$F_{CO,CO,cis}$	0.11	0.09	0.09	0.03	0.02	0.03	0.00	0.01
	$F_{CO,CO,trans}$	0.11	0.08	0.08	0.02	0.02	0.02	−0.01	0.00

[a] Calculated at BP86/ECP2. F_{MCO} = in molecular plane; F'_{MCO} = perpendicular to molecular plane; see text for units.

TABLE 12: ^{13}CO and $C^{18}O$ Isotopic Shifts (in cm^{-1}) for $[Au(CO)_2]^+$

			^{13}CO exptl[a]	^{13}CO calcd	$C^{18}O$ exptl[a]	$C^{18}O$ calcd
Σ_g+	ν_1	[CO]	51.5	52.9	49	49.5
Σ_g+	ν_2	[MC]	6.5[b]	6.5	10[b]	14.6
Σ_u+	ν_3	[CO]	50.5	50.1	52	51.2
Σ_u+	ν_4	[MC]	4.5	4.7	9	9.8
Π_g	ν_5	[δMCO]	9.0	8.9	3.5	3.9
Π_u	ν_6	[δMCO]	14	13.1	3	2.9
Π_u	ν_7	[δCMC]	0	0.1	5	2.5

[a] Values for solid $[Au(CO)_2][Sb_2F_{11}]$; ref 41b. Calculated values at BP86/ECP2. [b] Calculated from $(\nu_2 + \nu_3) - \nu_3$, see ref 41b.

stants for all 3d complexes where data on all four levels are available (314 data points; see Figures S1 and S2 in the Supporting Information), the agreement is excellent over the whole range of force constants. However, there is some scatter of the data points in the M−C stretching region, which may be related to the small differences in the calculated M−C bond lengths between the AE and ECP calculations.

The correlation between the BP86/ECP1 and MP2/ECP1 force constants for all neutral 4d and 5d carbonyls (176 data points; see Figures S3 and S4 in the Supporting Information) is still satisfactory, although there is much more scatter than in the other plots. The largest discrepancies are found in the C−O stretching region for $Pd(CO)_4$ and $Pt(CO)_4$ and in the M−C stretching region for $Ru(CO)_5$ and $Os(CO)_5$.

4. Discussion

In this section, we address the variation of the calculated force constants (BP86/ECP2) within the three series $[M(CO)_6]^n$ (six molecules, total charge n between 0 and 5), $[M(CO)_4]^n$ (four molecules, total charge n between 1 and 4), and $[M(CO)_2]^n$ (three molecules, total charge n between 1 and 3). For the hexa- and tetracarbonyl series, we will focus on the 5d complexes since the results for the respective 3d and 4d complexes are very similar. Figure 3 shows the change in the C−O stretching force constants F_{CO} as a function of n (Tables 10, 11, and 13) for all 5d complexes except $[Ta(CO)_6]^-$. Figure 4 displays the analogous M−C force constants F_{MC}. Figures 5 and 6 show the calculated C−O and M−C bond lengths at BP86/ECP2.[3,6,7]

TABLE 13: Harmonic Symmetry Force Constants F_{ij} and Internal Force Constants F_{int} for the 5d Complexes $[M(CO)_2]^n$ (M = Au, Hg, Tl; n = 1 to 3, respectively)

		M = Au		M = Hg	M = Tl
		exptl[a] (solid)	BP86 ECP2	BP86 ECP2	BP86 ECP2
Σ_g+	$F_{1,1}$	20.25 ± 0.1	19.51	20.49	20.16
	$F_{1,2}$	0.45 ± 0.2	0.20	−0.06	−0.16
	$F_{2,2}$	2.70 ± 0.03	2.80	1.74	1.09
Σ_u+	$F_{3,3}$	19.95 ± 0.1	19.42	20.49	20.17
	$F_{3,4}$	0.45 ± 0.2	0.41	−0.02	−0.08
	$F_{4,4}$	1.62 ± 0.03	1.67	1.62	1.43
Π_g	$F_{5,5}$	0.253 ± 0.02	0.25	0.22	0.22
Π_u	$F_{6,6}$	0.283 ± 0.02	0.28	0.23	0.22
	$F_{6,7}$	−0.02 ± 0.02	−0.12	−0.06	−0.03
	$F_{7,7}$	0.77 ± 0.09	0.31	0.32	0.26
	F_{CO}	20.1 ± 0.1	19.46	20.49	20.17
	F_{MC}	2.16 ± 0.03	2.24	1.68	1.26
	F_{MCO}	0.268 ± 0.02	0.26	0.23	0.22
	$F_{CO,CO'}$	0.15 ± 0.1	0.05	0.00	0.00

[a] Reference 41b; calculated from internal force constants; see also ref 45. $F_{7,7} = F_{CMC}$; see text for units.

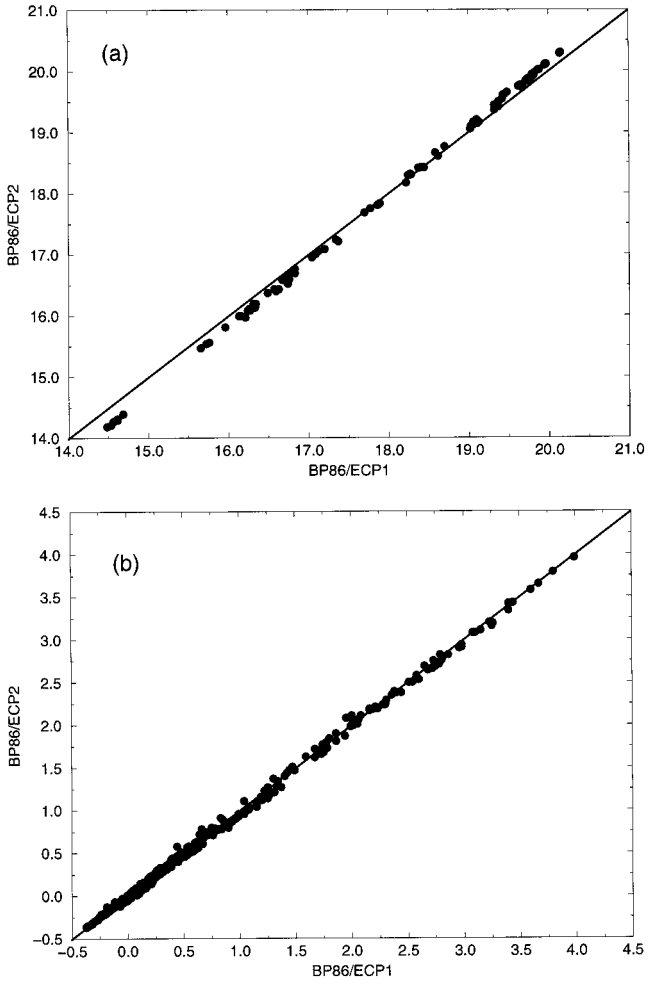

Figure 2. BP86/ECP2 versus BP86/ECP1 force constants for series (a−e), divided into two regions (a) (C−O stretches) and (b) (M−C stretches, all bends and coupling constants). The correlation lines with unit slope are shown; see text for units.

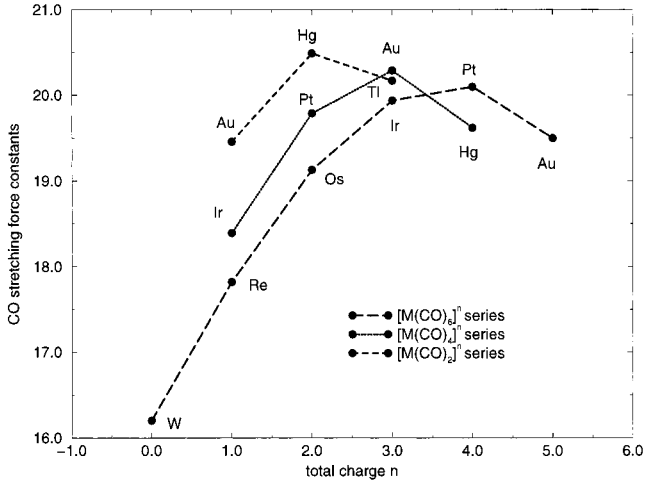

Figure 3. CO stretching force constants (in mdyn Å^{-1}) versus total charge n for $W(CO)_6$ and all 5d carbonyl cations.

F_{CO} increases significantly in all three series with increasing n up to $n = 4$ (M = Pt) for the hexacarbonyls, $n = 3$ (M = Au) for the tetracarbonyls, and $n = 2$ (M = Hg) for the dicarbonyls. The analogous inverse trend can be seen in the C−O bond lengths, which have the lowest values in each series for the same molecules (1.1217 Å for $[Pt(CO)_6]^{4+}$, 1.1206 Å for $[Au(CO)_4]^{3+}$, and 1.1196 Å for $[Hg(CO)_2]^{2+}$).[3,6,7] The calculated

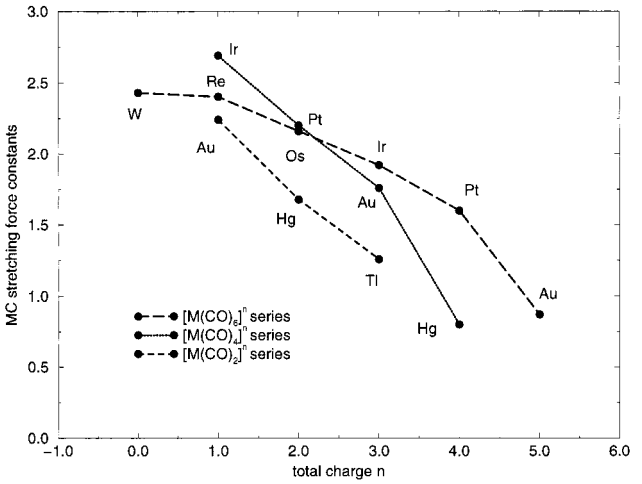

Figure 4. MC stretching force constants (in mdyn Å^{-1}) versus total charge n for $W(CO)_6$ and all 5d carbonyl cations.

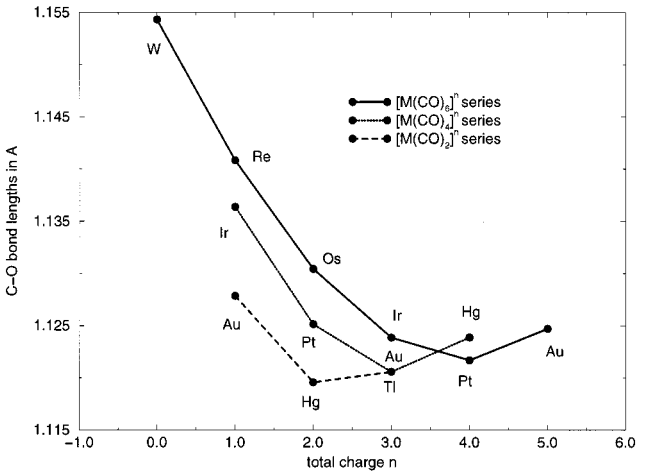

Figure 5. CO bond lengths (in Å) versus total charge n for $W(CO)_6$ and all 5d carbonyl cations.

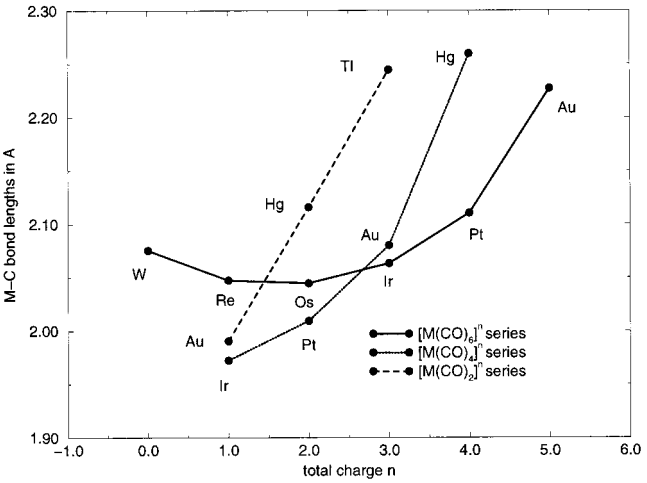

Figure 6. MC bond lengths (in Å) versus total charge n for $W(CO)_6$ and all 5d carbonyl cations.

M−C force constants decrease gradually for all three series with increasing total charge n (Figure 4). The values for the cations with the highest C−O force constants are not very different: 1.68 mdyn/Å for the known $[Hg(CO)_2]^{2+}$;[46] 1.76 mdyn/Å for the unknown $[Au(CO)_4]^{3+}$; 1.60 mdyn/Å for the unknown $[Pt(CO)_6]^{4+}$. The corresponding M−C bond lengths are also similar: 2.1105 Å for $[Pt(CO)_6]^{4+}$; 2.0800 Å for $[Au(CO)_4]^{3+}$;

TABLE 14: F_{CO} and $F_{CO,CO}$ Force Constants (in mdyn Å^{-1}) for Experimentally Known Carbonyl Complexes

	F_{CO} CK[a]	$F_{CO,CO}$ (cis) CK[a]	$F_{CO,CO}$ (trans) CK[a]	F_{CO} BP86[b]	$F_{CO,CO}$ (cis) BP86[b]	$F_{CO,CO}$ (trans) BP86[b]
$[V(CO)_6]^-$	14.55	0.33	0.60	14.47	0.23	0.19
$[Cr(CO)_6]$[c]	16.64	0.26	0.48	16.27	0.17	0.14
$[Mo(CO)_6]$[c]	16.66	0.27	0.45	16.30	0.16	0.12
$[W(CO)_6]$[c]	16.60	0.29	0.48	16.20	0.16	0.11
$[Cr(CO)_6]$[d]	16.45	0.26	0.54			
$[Mo(CO)_6]$[d]	16.46	0.27	0.54			
$[W(CO)_6]$[d]	16.35	0.30	0.57			
$[Mn(CO)_6]^+$	18.17	0.19	0.45	17.92	0.10	0.09
$[Re(CO)_6]^+$	18.09	0.22	0.53	17.82	0.10	0.07
$[Fe(CO)_6]^{2+}$	19.82	0.06	0.21	19.20	0.05	0.03
$[Ru(CO)_6]^{2+}$	19.83	0.10	0.30	19.22	0.05	0.03
$[Os(CO)_6]^{2+}$	19.74	0.12	0.37	19.13	0.05	0.03
$[Ir(CO)_6]^{3+}$	20.78	0.06	0.20	19.94	0.02	0.00
$[Rh(CO)_4]^+$	19.00	0.17	0.49	18.50	0.09	0.08
$[Pd(CO)_4]^{2+}$	20.61	0.07	0.21	19.86	0.02	0.02
$[Pt(CO)_4]^{2+}$	20.65	0.10	0.31	19.79	0.03	0.02
$[Au(CO)_2]^+$	20.18		0.33	19.46		0.05
$[Hg(CO)_2]^{2+}$	20.98		0.03	20.49		0.00

[a] Calculated from the experimental frequencies with the CK method; refs 2 and 5−7. [b] BP86/ECP2 values. [c] On the basis of gas-phase frequencies. [d] On the basis of solution frequencies.

2.1159 Å for $[Hg(CO)_2]^{2+}$; whereas for the next member of each series, the M−C bond length exceeds 2.22 Å.[47] From the point of view of the calculated bond lengths and force constants, there is no reason $[Au(CO)_4]^{3+}$ and $[Pt(CO)_6]^{4+}$ should not exist.

The experimental determination of C−O stretching force constants with the Cotton−Kraihanzel (CK) method has a long tradition in transition metal carbonyl chemistry.[2] In this approach, any coupling between C−O stretching and other modes is neglected and the observed frequencies are used without correcting for anharmonicity effects. One of the motivations for such empirical normal coordinate analysis is to explain the bonding and electronic structure of metal−CO complexes on the basis of force constants and vibrational frequencies. In this context, the Dewar−Chatt−Duncanson model[48] with σ donation from the CO lone pair into an empty metal d_σ orbital and π back-donation from filled metal d_π orbitals into the antibonding π^* orbital of CO is usually applied. This model should also be relevant for homoleptic carbonyl cations,[49] in principle, even though it is qualitatively clear that π back-donation will be less important and that electrostatic effects will be strong or even dominant in these cations, as has been shown before.[5,38,39,50]

Table 14 compares the F_{CO} and $F_{CO,CO}$ force constants from our BP86/ECP2 calculations with the respective CK values[2] for those members of the three series of carbonyl cations where the experimental CO frequencies are completely known.[5−7]

As expected from the frequencies, the BP86/ECP2 values for F_{CO} are consistently lower than the CK values. However, the overall variation of F_{CO} with the total charge is always reproduced nicely, as well as the variations within a group. On the basis of qualitative orbital arguments, CK have suggested[2] that the interaction constants $F_{CO,CO,cis}$ and $F_{CO,CO,trans}$ should be positive, which is confirmed in all cases (Table 14). Moreover, CK have argued that $F_{CO,CO,trans}$ should be twice as large as $F_{CO,CO,cis}$. The empirical CK values for these constants obey this rule only approximately, with $F_{CO,CO,cis} < F_{CO,CO,trans}$, whereas the opposite relation holds for the BP86/ECP2 values. The latter are generally smaller than their CK counterparts, especially in the case of $F_{CO,CO,trans}$ (Table 14). Since the theoretical interaction constants are normally quite reliable, this casts some doubt on the applicability of the CK treatment.

To clarify these inconsistencies, we consider the results for $W(CO)_6$ in more detail (Table 15). The experimental gas-phase C−O frequencies are well reproduced by the full BP86 calculations, with a uniform underestimate of 20−32 cm^{-1}. Applying the CK approximations[2] to the theoretical BP86 results (i.e., neglecting the kinetic energy and potential energy coupling between C−O and other modes) changes the C−O frequencies significantly, however, with nonuniform shifts ranging between −50 and +19 cm^{-1} (see last two columns in Table 15). In the CK treatment,[2] the internal force constants are proportional to the following quantities:

TABLE 15: Vibrational C−O Frequencies (in cm^{-1}) for $W(CO)_6$

	exptl ν_i[a] (vapor)	BP86[b] full	BP86[c] CK	BP86[d] shift
A_{1g}	2126.2	2094.7	2048.6	−50.1
E_g	2021.1	1998.8	1989.8	− 9.0
T_{1u}	1997.6	1977.1	1995.6	+18.5
ν_{av}[e]	2026.9	2003.3	2002.5	− 0.8
$\Delta\nu_1$[e]	17.5	16.0	9.8	− 6.2
$\Delta\nu_2$[e]	29.3	26.2	6.9	−19.3

[a] Reference 8. [b] BP86/ECP2 values. [c] Computed from the BP86 internal force constants (Table 14) by applying the CK approximations.[2] [d] Difference between the preceding two columns. [e] See text, eqs 1−3.

$$(1)\ F_{CO} \sim \nu_{av} = [\nu(A_{1g}) + 2\nu(E_g) + 3\nu(T_{1u})]/6$$

$$(2)\ F_{CO,CO,cis} \sim \Delta\nu_1 = [\nu(A_{1g}) - \nu(E_g)]/6$$

$$(3)\ F_{CO,CO,trans} \sim \Delta\nu_2 = \nu_{av} - \nu(T_{1u})$$

It is obvious from Table 15 that the CK approximations do not affect the average C−O frequency much (ν_{av}) but that they reduce the splittings strongly ($\Delta\nu_1$ and particularly $\Delta\nu_2$). Therefore, in such cases, the CK method will provide unphysical interaction force constants that deviate systematically from the true values (see Table 14).

Figure 7 shows the three C−O symmetry force constants and the internal C−O force constant for the hexacarbonyls. Since the interaction force constants are always positive, with $F_{CO,CO,cis} > F_{CO,CO,trans}$ (BP86/ECP2), the force constants are always in the order F_{11} (A_{1g}) > F_{CO} > F_{33} (E_g) > F_{66} (T_{1u}). The splitting becomes progressively less important with increasing total charge n, parallel to the decrease of π back-donation, which is reflected in decreasing interaction force constants. For $[Ir(CO)_6]^{3+}$, the cis interaction constant (0.02 mdyn/Å) still causes

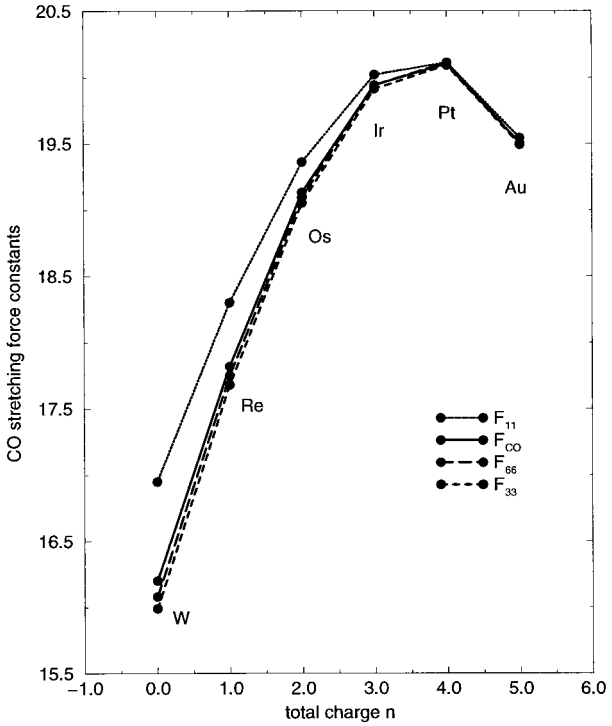

Figure 7. Diagonal symmetry and internal CO force constants (in mdyn Å^{-1}) versus total charge *n* for the hexacarbonyls $[M(CO)_6]^n$ (M = W, Re, Os, Ir, Pt, Au).

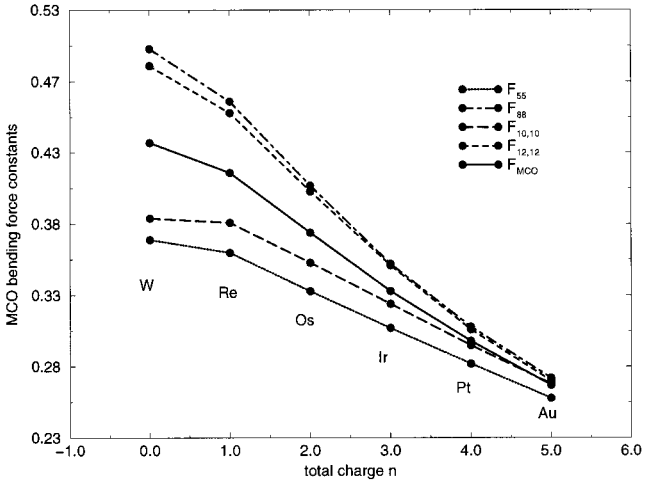

Figure 8. Diagonal symmetry and internal MCO bending force constants (in mdyn Å rad^{-2}) versus total charge *n* for the hexacarbonyls $[M(CO)_6]$ (M = W, Re, Os, Ir, Pt, Au).

a visible splitting between the different symmetry force constants (Figure 7), whereas for $[Pt(CO)_6]^{4+}$, the interaction elements approach zero and the splitting has disappeared. The analogous trends of interaction elements are seen in the tetracarbonyl series (Table 11) where the interaction elements are 0.03 mdyn/Å ($F_{CO,CO,cis}$) and 0.02 mdyn/Å ($F_{CO,CO,trans}$) for $[Pt(CO)_4]^{2+}$ and approach zero for the triply charged $[Au(CO)_4]^{3+}$. Thus, π back-donation becomes negligible for the highly charged cations.

Another indication for the diminishing π back-donation comes from the changes in the M−C−O bending vibrations with increasing total charge *n*. Figure 8 displays the corresponding bending force constants F_{55}, F_{88}, $F_{10,10}$, $F_{12,12}$, and F_{MCO} for the hexacarbonyls.

π back-donation is expected to stiffen the linear M−C−O moiety, thus leading to higher bending frequencies and force constants for lower total charge *n*. The trend in all M−C−O force constants is obvious, all five values increase continuously with decreasing charge *n*. Generally, the symmetry force constants for the ungerade modes (F_{88} and $F_{12,12}$) are higher than F_{MCO}, whereas those for the gerade modes (F_{55} and $F_{10,10}$) are lower. The four symmetry force constants approach the internal force constant F_{MCO} with increasing *n*. According to the expressions for the four symmetry constants in terms of internal constants,[8] this can be attributed to the bending interaction elements $F_{\beta\beta'}$, $F_{\beta\beta''}$, and $F_{\beta\beta'''}$ between pairs of CO groups, where for all members in the hexacarbonyl series the trans interaction element $F_{\beta\beta'}$ is much larger than the other two. $F_{\beta\beta'}$ diminishes from 0.06 for $W(CO)_6$ to 0.004 for $[Au(CO)_6]^{5+}$. The effect of $F_{\beta\beta'}$ can be understood qualitatively; in the two ungerade vibrations, two trans CO ligands vibrate in the same direction, whereas in the two gerade vibrations, they vibrate in opposite directions. The higher energy of the ungerade distortions is directly related to the π back-donation in the subunit O═C−M−C═O, since the motion of the two carbons in the same direction costs more energy than the motion in the opposite direction because the linearity of C−M−C is preserved more in the latter case.

For the tetracarbonyl series $[M(CO)_4]^n$ and the dicarbonyl series $[M(CO)_2]^n$, the same behavior of the M−C−O bending force constants with increasing charge *n* is found concerning the gerade and ungerade vibrations. Again, the differences between the symmetry force constants for gerade and ungerade modes get systematically smaller with increasing *n*. For the dicarbonyls, this difference is directly related to the single coupling constant $F_{\beta\beta'}$ which is 0.014 for M = Au, 0.006 for M = Hg, and 0.003 for M = Tl.

Among the cations that are experimentally known by now,[49] it is only for the dicarbonyls that the complex with the highest calculated C−O force constant and the shortest C−O bond length, i.e., $[Hg(CO)_2]^{2+}$, is known.[46] On the basis of the calculated force constants and geometries, there is no reason $[Au(CO)_4]^{3+}$ and $[Pt(CO)_6]^{4+}$ should not exist as homologues of $[Pt(CO)_4]^{2+}$ and $[Ir(CO)_6]^{3+}$.[51,52] The highest experimentally observed C−O stretching frequency has been reported for $[Ir(CO)_6]^{3+}$ (A_{1g}, 2295 cm^{-1}),[52] which exceeds those for $[Hg(CO)_2]^{2+}$ (Σ_g^+, 2282 cm^{-1})[46] and $[Pt(CO)_4]^{2+}$ (A_{1g}, 2289 cm^{-1})[51] because of the larger splittings of the C−O stretches in an octahedral complex. Correcting for systematic errors in the BP86/ECP2 results,[5,6] we expect still higher C−O frequencies for the A_{1g} modes in $[Pt(CO)_6]^{4+}$ and $[Au(CO)_4]^{3+}$ (around 2296 and 2306 cm^{-1}, respectively).

5. Concluding Remarks

Comparisons with experiment and the consistency of the theoretical results at different levels indicate that BP86/ECP2 density functional calculations provide reliable harmonic force fields both for neutral and charged transition metal carbonyls. The trends in the computed force constants can be understood in terms of σ donation, π back-donation, and electrostatic effects. The variations in the C−O stretching, CO−CO coupling, and M−C−O bending force constants show, in particular, that π back-donation effectively vanishes with increasing total charge and that electrostatic effects become dominant in the highly charged cations. The empirical Cotton−Kraihanzel approach captures trends in the C−O stretching force constants well but does not yield reliable cis and trans CO−CO interaction constants.

Acknowledgment. This work was supported by the Schweizerischer Nationalfonds. The calculations were carried

out using IBM RS/6000 workstations at the University Zürich and ETH Zürich (C4 Cluster) as well as the NEC SX-4 computer at CSCS Manno. We thank Dr. W. D. Allen (University of Georgia, Athens) for a copy of the INTDER program.

Supporting Information Available: Tables S1−S4 contain the complete symmetry coordinates for $[M(CO)_6]$ (O_h symmetry), $[M(CO)_5]$ (D_{3h} symmetry), $[M(CO)_4]$ (D_{4h} symmetry), and $[M(CO)_2]$ ($D_{\infty h}$ symmetry); Table S5 lists the calculated structures, frequencies, and infrared intensities for $[V(CO)_6]^-$, $[Mn(CO)_6]^+$, and $[Fe(CO)_6]^{2+}$ at the BP86/AE1 and BP86/AE2 levels of theory; Tables S6−S8 present the symmetry force fields for the neutral transition metal carbonyls $[M(CO)_6]$ (M = Cr, Mo, W), $[M(CO)_5]$ (M = Fe, Ru, Os), and $[M(CO)_4]$ (M = Ni, Pd, Pt) at the BP86/AE1 (M = Cr, Fe, Ni), BP86/AE2 (M = Cr, Fe, Ni), BP86/ECP1 (all nine complexes), and MP2/ECP1 (M = Mo, W, Ru, Os, Pd, Pt) levels of theory; Tables S9 and S10 contain the symmetry force fields for the isoelectronic hexacarbonyl ions $[M(CO)_6]^n$ (M = V, Nb, Ta; Mn, Re; Fe, Ru, Os; Co, Rh, Ir; Pt; Au; $n = -1$ to 5, respectively) at the BP86/AE1 (M = V, Mn, Fe), BP86/AE2 (M = V, Mn, Fe), and BP86/ECP1 (all complexes) levels of theory. Table S11 lists the symmetry force fields for the isoelectronic tetracarbonyl ions $[M(CO)_4]^n$ (M = Co, Rh, Ir; Ni, Pd, Pt; Au; Hg; $n = 1-4$, respectively) at the BP86/ECP1 level of theory; Table S12 shows the theoretical and experimental ^{13}CO and $C^{18}O$ isotopic shifts for $Ru(CO)_5$, $Os(CO)_5$, $Pd(CO)_4$, and $Pt(CO)_4$ at BP86/ECP2; Table S13 contains the theoretical and experimental ^{13}CO isotopic shifts for $[M(CO)_6]^n$ (M = Mn, Re; Fe, Ru, Os; Co, Rh, Ir; Pt; Au) at BP86/ECP2; Figures S1 and S2 show plots of BP86/ECP1 and BP86/ECP2 versus BP86/AE1 and BP86/AE2 force constants for the 3d complexes $[M(CO)_6]^n$ (M = V, Cr, Mn, Fe; $n = -1$ to 2, respectively), $M(CO)_5$, and $Ni(CO)_4$; Figures S3 and S4 display MP2/ECP1 versus BP86/ECP1 force constants for all neutral 4d and 5d carbonyls. This material is available free of charge via the Internet at http://pubs.acs.org.

References and Notes

(1) Fogarasi, G.; Pulay, P. In *Vibrational Spectra and Structure*; Durig, J. R., Ed.; Elsevier: Amsterdam, 1985; Vol. 14, pp 125−219.

(2) Cotton, F. A.; Kraihanzel, C. S. *J. Am. Chem. Soc.* **1962**, *84*, 4432.

(3) Jonas, V.; Thiel, W. *J. Chem. Phys.* **1995**, *102*, 8474.

(4) Jonas, V.; Thiel, W. *J. Chem. Phys.* **1996**, *105*, 3636.

(5) Jonas, V.; Thiel, W. *Organometallics* **1998**, *17*, 353.

(6) Bach, C.; Balzer, G.; Willner, H.; Aubke, F.; Jonas, V.; Thiel, W. To be submitted.

(7) Jonas, V.; Thiel, W. To be submitted.

(8) Jones, L. H.; McDowell, R. S.; Goldblatt, M. *Inorg. Chem.* **1969**, *8*, 2349.

(9) Jones, L. H.; McDowell, R. S.; Goldblatt, M.; Swanson, B. I. *J. Chem. Phys.* **1972**, *57*, 2050.

(10) Hedberg, L.; Iijima, T.; Hedberg, K. *J. Chem. Phys.* **1979**, *70*, 3224.

(11) (a) Jones, L. H.; McDowell, R. S.; Goldblatt, M. *J. Chem. Phys.* **1968**, *48*, 2663. (b) Jones, L. H.; McDowell, R. S.; Swanson, B. I. *J. Chem. Phys.* **1973**, *58*, 3757.

(12) Frisch, M. J.; Trucks, G. W.; Schlegel, H. B.; Gill, P. M. W.; Johnson, B. G.; Robb, M. A.; Cheeseman, J. R.; Keith, T.; Petersson, G. A.; Montgomery, J. A.; Raghavachari, K.; Al-Laham, M. A.; Zakrzewski, V. G.; Ortiz, J. V.; Foresman, J. B.; Cioslowski, J.; Stefanov, B. B.; Nanayakkara, A.; Challacombe, M.; Peng, C. Y.; Ayala, P. Y.; Chen, W.; Wong, M. W.; Andres, J. L.; Replogle, E. S.; Gomperts, R.; Martin, R. L.; Fox, D. J.; Binkley, J. S.; Defrees, D. J.; Baker, J.; Stewart, J. P.; Head-Gordon, M.; Gonzalez, C.; Pople, J. A. *Gaussian 94*, revision D.4; Gaussian, Inc.: Pittsburgh, PA, 1995.

(13) Becke, A. D. *Phys. Rev. A* **1988**, *38*, 3098.

(14) Perdew, J. P. *Phys. Rev. B* **1986**, *33*, 8822; (erratum) **1986**, *34*, 7406.

(15) Møller, C.; Plesset, M. S. *Phys. Rev.* **1934**, *46*, 618.

(16) Wachters, A. J. H. *J. Chem. Phys.* **1970**, *52*, 1033.

(17) Hay, P. J. *J. Chem. Phys.* **1977**, *66*, 4377.

(18) (a) Dolg, M.; Wedig, U.; Stoll, H.; Preuss, H. *J. Chem. Phys.* **1987**, *86*, 866. (b) Andrae, D.; Häussermann, U.; Dolg, M.; Stoll, H.; Preuss, H. *Theor. Chim. Acta* **1990**, *77*, 123.

(19) (a) Leininger, T.; Berning, A.; Nicklass, A.; Stoll, H.; Werner, H.-J.; Flad, H.-J. *Chem. Phys.* **1997**, *217*, 19. (b) www.theochem.uni-stuttgart.de and private communication H. Stoll, Stuttgart. From the original uncontracted (12s12p8d) basis set for Tl, the outermost diffuse s and p functions were deleted. The innermost six s, six p, and five d primitives were contracted to represent the doubly occupied $5s^25p^65d^{10}$ orbitals from a HF calculation on the Tl^{3+} ion.

(20) (a) Hehre, W. J.; Ditchfield, R.; Pople, J. A. *J. Chem. Phys.* **1972**, *56*, 2257. (b) Hariharan, P. C.; Pople, J. A. *Theor. Chim. Acta* **1973**, *28*, 213.

(21) Dunning, T. H. *J. Chem. Phys.* **1971**, *55*, 716.

(22) Dunning, T. H. *J. Chem. Phys.* **1989**, *90*, 1007.

(23) Johnson, B. G.; Frisch, M. J. *J. Chem. Phys.* **1994**, *100*, 7429.

(24) INTDER95 is a general program developed by Wesley D. Allen and co-workers that performs various vibrational analyses and higher order nonlinear transformations among force field representations. At the harmonic level, the transformations are elementary and involve standard B-matrix techniques; see, e.g., ref 1, pp 148−152 and the following: (a) Wilson, E. B., Jr.; Decius, J. C.; Cross, P. C. *Molecular Vibrations*; McGraw-Hill: New York, 1955. (b) Califano, S. *Vibrational States*; Wiley: New York, 1976.

(25) Huber, K. P.; Herzberg, G. P. *Constants of Diatomic Molecules*; Van Nostrand Reinhold: New York, 1979.

(26) Fan, L.; Ziegler, T. *J. Phys. Chem.* **1992**, *96*, 6937.

(27) Bérces A.; Ziegler, T. *J. Phys. Chem.* **1994**, *98*, 13233.

(28) Bérces A.; Ziegler, T. *J. Phys. Chem.* **1995**, *99*, 11417.

(29) Bérces A. *J. Phys. Chem.* **1996**, *100*, 16538.

(30) There are numerical problems in the BP86/AE1 calculation for $Fe(CO)_5$ (close coincidence of ν_4 and ν_{13}, which resulted in numerical instability of the corresponding intensities) when using the standard (75, 302) integration grid. The results given refer to the (85, 434) integration grid.

(31) (a) Adams, D. M.; Fernando, W. S.; Hooper, M. A. *J. Chem. Soc., Dalton Trans.* **1973**, 2264. (b) Afiz, M. R.; Clark, R. J. H.; D'Urso, N. R. *J. Chem. Soc., Dalton Trans.* **1977**, 250.

(32) The calculated Raman intensities for $Cr(CO)_6$ at BP86/AE1 are 70.6 (ν_1), 49.1 (ν_2), 202.6 (ν_3), 20.1 (ν_4), 0.7 (ν_{10}), 27.3 (ν_{11}), all values in $Å^4$/amu.

(33) Gregory, M. F.; Poliakoff, M.; Turner, J. J. *J. Mol. Struct.* **1985**, *127*, 247.

(34) Carsky, P.; Dedieu, A. *Chem. Phys.* **1986**, *103*, 265.

(35) (a) Jones, L. H. *J. Chem. Phys.* **1958**, *28*, 1215. (b) Crawford, B. L.; Horwitz, W. *J. Chem. Phys.* **1948**, *16*, 147.

(36) Kündig, P.; Moskovits, M.; Ozin, G. A. *J. Mol. Struct.* **1972**, *14*, 137.

(37) Ehlers, A. W.; Ruiz-Morales, Y.; Baerends, E. J.; Ziegler, T. *Inorg. Chem.* **1997**, *36*, 5031.

(38) Szilagyi, R. K.; Frenking, G. *Organometallics* **1997**, *16*, 4807.

(39) Lupinetti, A. J.; Fau, S.; Frenking, G.; Strauss, S. H. *J. Phys. Chem. A* **1997**, *101*, 9551.

(40) Goebel, S.; Haynes, C. L.; Khan, F. A.; Armentrout, P. B. *J. Am. Chem. Soc.* **1995**, *117*, 6994.

(41) (a) Willner, H.; Aubke, F. *Inorg. Chem.* **1990**, *29*, 2195. (b) Willner, H.; Schaebs, J.; Hwang, G.; Mistry, F.; Jones, R.; Trotter, J.; Aubke, F. *J. Am. Chem. Soc.* **1992**, *114*, 8972.

(42) Lupinetti, A. J.; Jonas, V.; Thiel, W.; Frenking, G.; Strauss, S. H., submitted.

(43) (a) Rack, J. J.; Webb, J. D.; Strauss, S. H. *Inorg. Chem.* **1996**, *35*, 277. (b) Hurlburt, P. K.; Rack, J. J.; Dec, S. F.; Anderson, O. P.; Strauss, S. H. *Inorg. Chem.* **1993**, *32*, 373. (c) Hurlburt, P. K.; Rack, J. J.; Luck, J. S.; Dec, S. F.; Webb, J. D.; Anderson, O. P.; Strauss, S. H. *J. Am. Chem. Soc.* **1994**, *116*, 10003.

(44) Meyer, F.; Chen, Y.-M.; Armentrout, P. B. *J. Am. Chem. Soc.* **1995**, *117*, 4071.

(45) Jones, L. H. *Inorganic Vibrational Spectroscopy*; Marcel Dekker: New York, 1971; p 117.

(46) (a) Willner, H.; Bodenbinder, M.; Wang, C.; Aubke, F. *J. Chem. Soc., Chem. Commun.* **1994**, 1189. (b) Bodenbinder, M.; Balzer-Jöllenbeck, G.; Willner, H.; Batchelor, R. J.; Einstein, F. W. B.; Wang, C.; Aubke, F. *Inorg. Chem.* **1996**, *35*, 82.

(47) For the next member of the hexacarbonyl series, i.e., $[Hg(CO)_6]^{6+}$, no minimum could be located.

(48) (a) Dewar, M. J. S. *Bull. Soc. Chim. Fr.* **1951**, *18*, C71. (b) Chatt, J.; Duncanson, L. A. *J. Chem. Soc.* **1953**, 2939.

(49) Willner, H.; Aubke, F. *Angew. Chem.* **1997**, *109*, 2506; *Angew. Chem., Int. Ed. Engl.* **1997**, *36*, 2402.

(50) Goldman, A. S.; Krogh-Jespersen, K. *J. Am. Chem. Soc.* **1996**, *118*, 12159.

(51) Hwang, G.; Bodenbinder, M.; Willner, H.; Aubke, F. *Inorg. Chem.* **1993**, *32*, 4667. (b) Hwang, G.; Wang, C.; Aubke, F.; Willner, H.; Bodenbinder, M. *Can. J. Chem.* **1993**, *71*, 1532.

(52) Bach, C.; Willner, H.; Wang, C.; Rettig, S. J.; Trotter, J.; Aubke, F. *Angew. Chem.* **1996**, *108*, 2104; *Angew. Chem., Int. Ed. Engl.* **1996**, *35*, 1974.

(53) (a) Darling, J. H.; Ogden, J. S. *Inorg. Chem.* **1972**, *11*, 666. (b) Kündig, E. P.; McIntosh, D.; Moskovits, M.; Ozin, G. A. *J. Am. Chem. Soc.* **1973**, *95*, 7234.

(54) (a) Bley, B.; Willner, H.; Aubke, F. *Inorg. Chem.* **1997**, *36*, 158. (b) Wang, C.; Bley, B.; Balzer-Jöllenbeck, G.; Lewis, A. R.; Siu, S. C.; Willner, H.; Aubke, F. *J. Chem. Soc., Chem. Commun.* **1995**, 2071.